AD

PSI-PR-94-26
August 1994

PAUL SCHERRER INSTITUT

Two-loop large top mass corrections to electroweak parameters: Analytic results valid for arbitrary Higgs mass

su 8943

J. Fleischer[a], O.V. Tarasov[a,b], F. Jegerlehner[b]

a Fakultät für Physik, Universität Bielefeld, D-33615 Bielefeld, Germany

b Paul Scherrer Institut, CH-5232 Villigen PSI, Switzerland

Paul Scherrer Institut
Würenlingen and Villigen
CH-5232 Villigen / PSI

Telephone 056 99 21 11
Telefax 056 98 23 27
Telex 82 74 14 psi ch

BI-TP-94/05
PSI-PR-94-26
August, 1994

Two-loop large top mass corrections to electroweak parameters: Analytic results valid for arbitrary Higgs mass

J. Fleischer, O. V. Tarasov [1,2]

Fakultät für Physik, Universität Bielefeld, D-33615 Bielefeld, Germany

F. Jegerlehner

Paul Scherrer Institute, CH-5232 Villigen PSI, Switzerland

Abstract

We present analytic results valid for arbitrary Higgs mass of the heavy top mass expansion at two-loop order as needed for precise predictions of electroweak observables. In particular we present a set of recurrence relations for diagrams with three masses at zero momentum, which allow to reduce the calculation to a few master integrals. Simple analytic expressions are obtained for the ρ–parameter and for the $Zb\bar{b}$–vertex. Results are presented for the on-shell and the $\overline{MS}$ definition of the top quark mass.

---

[1]) Supported by Bundesministerium für Forschung und Technologie.

[2]) On leave of absence from Joint Institute for Nuclear Research, Dubna, 101 000 Moscow, Russian Federation.

1. Introduction

Continuous progress in the accuracy of experiments at the e^+e^- colliders LEP at CERN [1] and SLC at SLAC [2] and the fact that no signs for deviations from the Standard Model (SM) have been seen so far are a strong motivation to lower further the theoretical uncertainties of SM predictions by performing higher order calculations. As experiments at the Z peak will go on for some time we can still hope that small deviations from the electroweak SM will show up.

The detailed investigation of $e^+e^- \to f\bar{f}$ around the Z resonance led to a very precise measurement of the Z–mass, which together with the fine structure constant α and the μ–decay constant G_μ provides a set of very accurate input parameters in terms of which precise predictions of the SM become possible. This allows us to confront accurate predictions with accurate measurements of the partial and total cross-sections $\sigma_f = \sigma(e^+e^- \to f\bar{f})$ and $\sigma_{tot} = \sum_f \sigma_f$ and the partial and total widths $\Gamma_f = \Gamma(Z \to f\bar{f})$ and $\Gamma_Z = \sum_f \Gamma_f$, for example. At lowest order the predictions for these quantities read

$$\sigma_f^{peak} = \frac{12\pi}{M_Z^2}\frac{\Gamma_e\Gamma_f}{\Gamma_Z^2} \;\; ; \;\; \Gamma_f = \frac{\sqrt{2}G_\mu M_Z^3}{12\pi}(v_f^2 + a_f^2)N_{cf}$$

where $v_f = T_{3f} - 2Q_f \sin^2\Theta_W$ and $a_f = T_{3f}$ are, respectively, the vector and axial-vector neutral current (NC) couplings for fermions with flavor f. N_{cf} is the color factor, which is 1 for leptons and 3 for quarks. We define $\sin^2\Theta_W = 1 - M_W^2/M_Z^2$ in terms of the intermediate vector boson masses.

Higher order corrections of the $Zf\bar{f}$ vertex

$$(-i)(\sqrt{2}G_\mu)^{1/2}M_Z\gamma^\mu(v_f - a_f\gamma_5)$$

can be cast into an overall renormalization by $\rho_f^{1/2}$ and a renormalization by κ_f of $\sin^2\Theta_W$ in the NC vector-couplings

$$\begin{aligned} G_\mu &\to \rho_f G_\mu \\ \sin^2\Theta_W &\to \kappa_f \sin^2\Theta_W \equiv \sin^2\Theta_{eff}^f(M_Z) \;\; . \end{aligned}$$

Here $\sin^2\Theta_{eff}^f(M_Z)$ is the weak mixing parameter effective at the Z resonance. Information on this parameter is obtained also from the on-resonance asymmetries, the forward-backward asymmetries $A_{FB}^{f\bar{f}}$, the τ polarization-asymmetry A_{pol}^τ. With longitudinally polarized beams, presently available at SLC only, the measurement of the left-right asymmetry A_{LR} and the polarized forward-backward asymmetries $A_{FB,pol}^{f\bar{f}}$ in principle allow for particularly clean tests of the SM. At tree level the on-resonance asymmetries are given by

$$A_{FB}^{f\bar{f}} = \frac{3}{4}A_eA_f, \;\; A_{LR} = A_{pol}^\tau = A_e, \;\; A_{FB,pol}^{f\bar{f}} = \frac{3}{4}A_f$$

in terms of the ratios

$$A_f = \frac{2v_fa_f}{v_f^2 + a_f^2}$$

of the NC couplings, and thus provide accurate determinations of $\sin^2\Theta^f_{eff}(M_Z)$. At present, the values determined by LEP [1] 0.2321±0.0004 and SLC [2] 0.2294±0.0010 (from A_{LR}) deviate by about 2.5 standard deviations.

In the coming years we expect that the experimental uncertainty $\delta\sin^2\Theta_{eff}(M_Z)$ can be reduced from 0.0006 at present to about 0.0004. Similarly, for the interesting channel $Z \to b\bar{b}$, the uncertainty $\delta\Gamma_{b\bar{b}}/\Gamma_{had}$ is expected to improve from 1.2% at present to about 0.5%. In addition, the CDF and D0 experiments at the Fermilab proton collider Tevatron will improve on the accuracy of the value for M_W/M_Z [3], which provides another important test of the SM.

For the physical interpretation of precision tests an important step forward is the direct production of the top quark and the determination of the top quark mass. CDF recently found evidence for top quark production and determined the value $174 \pm 10^{+13}_{-12}$ GeV for the top quark mass [4]. This is a surprisingly large value which is in accord, however, with the indirect bounds which were obtained by LEP previously.

Many predictions of electroweak observables depend substantially on the top mass. They are affected by corrections which are proportional to $G_\mu m_t^2$, at the one–loop level, as a consequence of the large top-bottom quark mass splitting. Since these corrections grow rapidly with m_t electroweak precision measurements allow to put stringent upper bounds on the top mass. The present constraint on the top mass from LEP $m_t = 173^{+12+18}_{-13-20}$ GeV, which assumes the Higgs mass in the range $m_H = 300^{+700}_{-240}$ GeV [1], is close to the CDF value mentioned above.

For four fermion processes the SM predicts two different sources of leading heavy top corrections; first the Z and W self-energies [5], second the $Z\bar{b}b$ vertex [6]. The former in particular modify the ρ-parameter defined by the neutral to charged current coupling ratio at low momentum transfer. The leading correction to ρ is contained in the contribution of the transversal parts of the gauge boson self-energies which enters all four fermion processes in a universal manner. This is different for the $Z\bar{b}b$ vertex, where the virtual top effect is tagged by the external b state. Top effects in ρ, and hence the top mass bounds, may be masked by all kind of contributions from non-standard physics. As already mentioned, the situation will change dramatically if the discovery of the top in Ref. [4] will be confirmed and m_t will be known more reliably. Hunting for small effects originating from the Higgs, from the gauge boson self-interaction or possible small contributions from new physics will then become much more transparent.

In any case a precise knowledge of heavy particle effects is important. Activities in this direction are of course not new. The high accuracy of LEP data has motivated increasing interest in this subject recently [7, 8, 9, 10].

We have performed an independent calculation of the leading two–loop heavy top mass effects for arbitrary Higgs mass which was presented previously in Ref. [8]. We were able to obtain simple analytic results and found numerical agreement with [8]. We directly calculated the physical W and Z amplitudes and explicitly checked the validity of the Ward-Takahashi identities on which the calculation of Ref. [8] was based. In this way we also could check directly that the use of an anticommuting γ_5 preserves the Ward identities.

Our main results were published in a letter [10], recently. Here we describe the calculation in some details, because we think that many technical aspects of our calculation might be interesting for other two-loop calculations. Also, for the purpose of direct comparisons, a more detailed presentation of our results should be useful for other authors.

In Section 2 we present our main results. An outline of the calculation is given in Section 3. Ward-Takahashi identities and renormalization are considered in Section 4 and detailed results follow in Section 5.

2. Results

1. Universal corrections from gauge boson self-energies to $\Delta\rho$

The ρ-parameter is defined by the neutral to charged current coupling ratio at low momentum transfer

$$\rho = \frac{G_{NC}(0)}{G_{CC}(0)} = \frac{1}{1-\Delta\rho} \tag{1}$$

where $G_{CC}(0) = G_\mu$ is the Fermi constant determined by the μ-decay rate. The leading correction to ρ stems from the transversal parts of the gauge boson self-energies

$$\Delta\rho = \frac{\Pi_Z(0)}{M_Z^2} - \frac{\Pi_W(0)}{M_W^2} \tag{2}$$

which enters all four fermion processes in a universal manner.

Some observables which are affected by $\Delta\rho$ are briefly mentioned here. One is the W-mass as predicted from α, G_μ and M_Z [11]

$$M_W^2 = \frac{\rho M_Z^2}{2}\left(1+\sqrt{1-\frac{4A_0^2}{\rho M_Z^2}\left(\frac{1}{1-\Delta\alpha}+\cdots\right)}\right) \tag{3}$$

where $A_0 = \left(\frac{\pi\alpha}{\sqrt{2}G_\mu}\right)^{1/2} = 37.2802(3)$ GeV and $\Delta\alpha \simeq 0.06$ is the shift of the finestructure constant α due to photon vacuum polarization effects. The ellipsis stands for the non-leading remainder terms. This relationship also determines the weak mixing parameter defined by $\sin^2\Theta_W = 1 - \frac{M_W^2}{M_Z^2}$ in terms of the physical vector boson masses. The other is the effective weak mixing parameter relevant for Z-resonance physics given by

$$\sin^2\Theta_{eff}(M_Z) = \kappa\sin^2\Theta_W = 1 - \frac{M_W^2}{\rho M_Z^2} = \frac{1}{2}\left(1-\sqrt{1-\frac{4A_0^2}{\rho M_Z^2}\left(\frac{1}{1-\Delta\alpha}+\cdots\right)}\right) \quad . \tag{4}$$

The leading contribution to the ρ–parameter in the large m_t limit may be written in the form

$$\Delta\rho = 1 - \frac{1}{\rho} = N_c\, x_t\,(\rho^{(1)} + x_t\,\rho^{(2)}) \;\; ; \;\; x_t = \frac{\sqrt{2}G_\mu m_t^2}{16\pi^2} \tag{5}$$

where $\rho^{(1)} = 1$ and $\rho^{(2)}$ is a function of the ratio of the squares of the Higgs and the top mass which we denote by

$$a = \frac{m_H^2}{m_t^2}$$

in the following.

Our result may be expressed in terms of the following three functions (see the Appendix):

$$f(a,1) \;=\; \begin{cases} -\frac{1}{\sqrt{1-y}}\left[\mathrm{Sp}\,(1)+2\,\mathrm{Sp}\,(\xi)+\frac{1}{2}\ln^2(-\xi)\right] & ;\;\; a \geq 4 \\ -\frac{2}{\sqrt{y-1}}\;\; C\ell_2\,(\varphi) & ;\;\; 4 \geq a \geq 0 \end{cases} \tag{6}$$

$$f(a,0) \;=\; \mathrm{Sp}\,(1-a) \;=\; \mathrm{Sp}\,(1) - \mathrm{Sp}\,(a) - \ln(a)\ln(1-a)\;\;, \tag{7}$$

and

$$g(a) = \begin{cases} \sqrt{a-4}\;\ln(-\xi) & \text{for} \quad a \geq 4 \\ \sqrt{4-a}\;(\pi-\varphi) & \text{for} \quad 0 \leq a \leq 4\;\;. \end{cases} \tag{8}$$

$\mathrm{Sp}\,(x) = -\int_0^1 \frac{dt}{t}\ln(1-xt)$ is the Spence function and $C\ell_2(\varphi) = \mathrm{Im}\;\mathrm{Sp}\,(e^{i\varphi})$ is the Clausen function. The kinematical variables ξ and φ are defined by

$$\xi \;=\; \frac{\sqrt{1-y}-1}{\sqrt{1-y}+1}\;\;;\quad y = 4a^{-1} \qquad \text{and} \qquad \varphi = 2\;\arcsin(\sqrt{\frac{a}{4}})\;\;, \tag{9}$$

respectively, and take the values

$$\begin{aligned} 0 \leq \xi \leq 1 \qquad & \text{for} \quad a \leq 0 \\ \xi = e^{i\varphi},\;\; 0 \leq \varphi \leq \pi \quad & \text{for} \quad 0 \leq a \leq 4 \\ -1 \leq \xi \leq 0 \qquad & \text{for} \quad 4 \leq a\;\;. \end{aligned}$$

For the dimensionally regularized quantities in $d = 4 - 2\varepsilon$ dimensions we will use the abbreviation

$$\frac{1}{\varepsilon} - \gamma + \ln\frac{4\pi\mu^2}{m_t^2} \to \frac{1}{\varepsilon}$$

in order to prevent uninteresting combinations of the Euler constant γ, $\ln 4\pi$ ... in intermediate results.

A direct calculation of Eq. (2) in terms of the gauge boson self–energies requires the calculation of the diagrams depicted in Figs. 1a and b. Collecting the contributions from the unrenormalized diagrams we find

$$\begin{aligned} \rho_B^{(2)} \;&=\; -\frac{3}{\varepsilon} + \frac{37}{2} - 3a - 3\,(2+a)\ln a + \frac{a-2}{2a}\pi^2 \\ &-\; \frac{3}{a}(a-1)^2(a-2)\;f(a,0) + 3\,(a^2-6a+10)\;f(a,1)\;\;. \end{aligned} \tag{10}$$

Since $\Delta\rho$ is finite at one loop order in the SM, it turns out that the only renormalization needed is due to the replacement of the bare top mass by the renormalized one. We use the on-shell

definition (pole mass) for m_t in the following. The contribution from the counterterm that must be added to $\rho_B^{(2)}$ is

$$\rho_{CT}^{(2)} = \frac{3}{\varepsilon} + \frac{13}{2} - a + \frac{a\,(a-6)}{2} \ln a + \frac{a-4}{2}\,\sqrt{a}\; g(a)\;\;, \tag{11}$$

and the sum of the two contributions yields

$$\begin{aligned} \rho^{(2)} \;&=\; 25 - 4a + \frac{1}{2}(a^2 - 12a - 12)\ln a + \frac{a-2}{2a}\pi^2 + \frac{1}{2}(a-4)\sqrt{a}\; g(a) \\ &-\; \frac{3}{a}(a-1)^2(a-2)\; f(a,0) + 3\,(a^2 - 6a + 10)\; f(a,1) \end{aligned} \tag{12}$$

as final result. This result confirms the numerical results and the asymptotic expansions given in Ref. [8]. The result depends substantially on the definition of the top quark mass. If we adopt the $\overline{MS}$ definition for the top quark mass and choose as a renormalization scale $\mu = m_t$ we obtain $\rho_{MS}^{(2)}$ by just dropping the ε–pole term in the bare result Eq. (10):

$$\begin{aligned} \rho_{MS}^{(2)} \;&=\; \frac{37}{2} - 3a - 3\,(2+a)\ln a + \frac{a-2}{2a}\pi^2 \\ &-\; \frac{3}{a}(a-1)^2(a-2)\; f(a,0) + 3\,(a^2 - 6a + 10)\; f(a,1)\;\;. \end{aligned} \tag{13}$$

The asymptotic expansions for large and small values of a, respectively, read:

$$\begin{aligned} \rho^{(2)} = \;& \ln^2 a\,(3/2 - 9\,a^{-1} - 15\,a^{-2} - 48\,a^{-3} - 168\,a^{-4} - 612\,a^{-5} + \cdots) \\ -\;& \ln a\,(27/2 + 4\,a^{-1} - 125/4\,a^{-2} - 558/5\,a^{-3} - 8307/20\,a^{-4} - 109321/70\,a^{-5} + \cdots) \\ +\;& \pi^2\,(1 - 4\,a^{-1} - 5\,a^{-2} - 16\,a^{-3} - 56\,a^{-4} - 204\,a^{-5} + \cdots) \\ +\;& 49/4 + 2/3\,a^{-1} + 1613/48\,a^{-2} + 8757/100\,a^{-3} + 341959/1200\,a^{-4} \\ +\;& 9737663/9800\,a^{-5} + \cdots \quad a \to \infty \end{aligned} \tag{14}$$

$$\begin{aligned} \rho^{(2)} = \;& -\ln a\,(3\,a - 1/2\,a^2 + \cdots) \\ -\;& \pi^2\,(2 - 2\,a + 1/2\,a^2) \\ -\;& \pi\sqrt{a}\,(4 - 3/2\,a + 3/32\,a^2 + 1/256\,a^3 + \cdots) \\ +\;& 19 - 33/2\,a + 43/12\,a^2 + 7/120\,a^3 + \cdots) \quad a \to 0\;\;. \end{aligned} \tag{15}$$

The correction $\rho^{(2)}$ is negative and thus leads to a screening of the non-decoupling large mass-splitting effects. The minimum screening of the doublet mass splitting $\Delta m_t^2 = |m_t^2 - m_b^2|$

$$\Delta\rho = N_c\, x_t\,[1 - (2\pi^2 - 19)\, x_t + \cdots]\;,\;\; x_t = \frac{\sqrt{2} G_\mu \Delta m_t^2}{16\pi^2}$$

is obtained for $m_H^2 \ll \Delta m_t^2$ [5, 7, 11].

The magnitude of the effect first increases with increasing Higgs mass and takes a maximum of about -11.77 at $m_H/m_t \simeq 5.7$. For asymptotically large m_H $\rho^{(2)} \sim 3/2 \ln^2 a$ is positive, but for reasonable values of m_H it is still negative. For $m_H/m_t = 10$ we have -10.74 still substantially larger than the value -0.74 at $m_H = 0$.

The somewhat unexpected shape (infinite derivative at $a = 0$) shown in Fig. 2a is due to the top mass renormalization counterterm Eq. (11) which exhibits a term proportional to $\sqrt{a}$ for small a. The non–monotonic behavior of $\rho^{(2)}$ is the result of a cancellation between the bare contribution which shows the expected smooth behavior (with zero derivative at $a = 0$) as a function of a and the top mass counter term which is also monotonic but decreasing. This is illustrated in Fig. 2b where $\rho^{(2)}_{CT}$ is subtracted at $a = 0$.

2. $Z \to b\bar{b}$ process specific vertex corrections

For physics at the Z–peak all corrections may be included into effective $Zf\bar{f}$-couplings like $|Q_f|\ \sin^2\Theta_f = |Q_f|\ \kappa_f \sin^2\Theta_W = \frac{1}{4}(1 - g^f_V/g^f_A)$ and $g^f_A = \rho_f\ T_{3f}$ which are determined by experiment [1, 2]. Accordingly we write the corrected vertex as [6]

$$(-i)\ \left(\sqrt{2}\,\rho_f\,G_\mu\right)^{1/2} M_Z\,\gamma^\mu\ \left(-2Q_f\kappa_f\ \sin^2\Theta_W - (1-\gamma_5)\,\frac{1}{2}\right) \tag{16}$$

where $\rho_f = \rho(1+\Delta\rho_{f,vertex})$ and $\kappa_f = \kappa(1+\Delta\kappa_{f,vertex})$. Here ρ and κ incorporate the universal self-energy corrections, discussed in the previous subsection, and the remaining terms the flavor dependent vertex corrections.

While for $f \neq b$ the vertex corrections are small and independent of m_t and m_H at one loop order, the $Z\bar{b}b$-vertex gets a process specific heavy top contribution proportional to $1-\gamma_5$ such that

$$\begin{aligned} \rho_b &= \rho\,(1+\tau_b)^2 \\ \kappa_b &= \kappa\,\frac{1}{1+\tau_b}\ . \end{aligned} \tag{17}$$

For large m_t we may write

$$\tau_b = -2x_t\,(\tau_b^{(1)} + x_t\,\tau_b^{(2)}) \tag{18}$$

where $\tau_b^{(1)} = 1$, x_t was defined in (5) and $\tau_b^{(2)}$ again is a function of a. Besides the asymmetries at the Z-resonance which are functions of $\sin^2\Theta^f_{eff}$ the heavy top contributions affect the partial Z-decay widths

$$\Gamma_{Z\to\bar{f}f} = \frac{\sqrt{2}G_\mu M_Z^3}{48\pi} N_{cf}\rho_f\ \left(1 + (1 - 4|Q_f|\,\kappa_f \sin^2\Theta_W)^2\right)\ . \tag{19}$$

For $f \neq b$ only the universal corrections ρ and κ enter which lead to a substantial top mass dependence. For $f = b$ the universal top mass dependence is largely cancelled by the τ_b correction.

The two–loop contribution $\tau_b^{(2)}$ was first calculated in Ref. [8]. The leading term for $a = 0$ was confirmed recently in Ref. [9]. We have performed an independent calculation of $\tau_b^{(2)}(a)$ and found a surprisingly simple analytic results. The Feynman diagrams which must be considered when doing a direct calculation of the $Zb\bar{b}$–vertex are shown in Figs. 3a and b. As for $\rho^{(2)}$, the

result can be written in a similar simple form in terms of the same basic functions. As a result we find

$$\tau_b^{(2)} = 9 - \frac{13}{4}a - 2a^2 - \frac{a}{4}(19+6a)\ln a - \frac{a^2}{4}(7-6a)\ln^2 a - (\frac{1}{4}+\frac{7}{2}a^2-3a^3)\frac{\pi^2}{6}$$
$$+ (\frac{a}{2}-2)\sqrt{a}\, g(a) + (a-1)^2(4a-\frac{7}{4})\, f(a,0) - (a^3 - \frac{33}{4}a^2 + 18a - 7)\, f(a,1)\,. \quad (20)$$

Our result reproduces the numerical results and the asymptotic expansions given in [8]. Again, the result depends substantially on the definition of the top quark mass. For the $\overline{MS}$ scheme at scale $\mu = m_t$ we obtain

$$\tau_{MS}^{(2)} = \frac{5}{2} - \frac{9}{4}a - 2a^2 - \frac{a}{4}(7+8a)\ln a - \frac{a^2}{4}(7-6a)\ln^2 a - (\frac{1}{4}+\frac{7}{2}a^2-3a^3)\frac{\pi^2}{6}$$
$$+ (a-1)^2(4a-\frac{7}{4})\, f(a,0) - (a^3 - \frac{33}{4}a^2 + 18a - 7)\, f(a,1)\,. \quad (21)$$

For large a the asymptotic expansion reads

$$\tau_b^{(2)} = (\frac{1}{6} - \frac{1}{6a} - \frac{5}{4a^2} - \frac{35}{6a^3})\pi^2$$
$$+ (\frac{5}{8} - \frac{1}{2a} - \frac{15}{4a^2} - \frac{35}{2a^3})\ln^2 a$$
$$+ (-\frac{47}{24} + \frac{5}{12a} + \frac{757}{80a^2} + \frac{5411}{120a^3})\ln a$$
$$+ \frac{311}{144} - \frac{10}{9a} + \frac{24209}{4800a^2} + \frac{193157}{7200a^3} + \cdots \quad a \to \infty \quad (22)$$

and for small a we obtain

$$\tau_b^{(2)} = (-4 + \frac{3}{2}a - \frac{3}{32}a^2 - \frac{1}{256}a^3)\sqrt{a}\pi$$
$$+ (-\frac{1}{3} + \frac{5}{4}a - \frac{53}{24}a^2 + \frac{7}{6}a^3)\pi^2$$
$$+ (-\frac{7}{4}a^2 + \frac{3}{2}a^3)\ln^2 a + (-3a - \frac{79}{24}a^2 - \frac{461}{120}a^3)\ln a$$
$$+ 9 - \frac{9}{2}a + \frac{955}{144}a^2 + \frac{164}{75}a^3 + \cdots \quad a \to 0\,. \quad (23)$$

The function $\tau_b^{(2)}(a)$ has a similar behavior as $\rho^{(2)}(a)$. In Fig. 4a we compare the exact result with the asymptotic expansions. Fig. 4b illustrates the role of the top mass counterterm. The remarks made earlier about the behavior of $\rho^{(2)}(a)$ apply for $\tau_b^{(2)}(a)$ as well.

3. Outline of the calculation, basic two-loop integrals

We are interested in corrections which grow at least as m_t^2 for asymptotically large top mass. At two-loops the leading term behaves like m_t^4. In a renormalizable theory (in a renormalizable gauge) if the masses would only enter via mass terms i.e. in propagators, we would have decoupling. The Feynman integrals would at most grow logarithmically in the mass. The origin of the above behavior clearly stems from the large Yukawa couplings $g_t = \frac{\sqrt{2}m_t}{v}$ of the top quark, the vacuum expectation value of the Higgs field v being fixed by the Fermi constant as $\frac{1}{v^2} = \sqrt{2}G_\mu$. Thus the diagrams we have to consider require at least two top Yukawa vertices $\bar{t}b\varphi^+$ and $\bar{b}t\varphi^-$ which are connected by at least one internal top line. As there are necessarily charged current transitions involved, the contributions will be purely left–handed. The other vertices representing large couplings are $\bar{t}t\varphi$ and $\bar{t}tH$, and, since the Higgs mass cannot be neglected, all the Higgs self-coupling vertices $H\varphi^+\varphi^-$, $H\varphi\varphi$, $H^2\varphi^+\varphi^-$, $\varphi^2\varphi^+\varphi^-$ and $(\varphi^+\varphi^-)^2$. The corresponding two–loop diagrams we have to consider are shown in Figs. 1 and 3. Using appropriate Ward-Takahashi identities the same results can be obtained form the diagrams depicted in Figs. 5 and 6, where the external gauge boson legs are replaced by corresponding Higgs ghost legs.

The calculation was done using dimensional regularization with anticommuting γ_5. The latter choice preserves the naive form of the Ward identities as we have checked explicitly. In the approximation studied we do not encounter any γ_5–odd traces which usually cause the triangle anomaly problem. All masses besides m_t and m_H are taken to be zero. Consistently with neglecting the vector boson masses also the momenta are taken to vanish. In this approximation all diagrams are effectively "vacuum bubble " diagrams corresponding to integrals of the form [12]

$$(m_{11},\, m_{12}\cdots m_{1n_1}|m_{21},\, m_{22}\cdots m_{2n_2}|m_{31},\, m_{32}\cdots m_{3n_3}) =$$
$$\int d^nk_1 \int d^nk_2 \prod_{i=1}^{n_1} \frac{1}{(k_1^2+m_{1i}^2)} \prod_{j=1}^{n_2} \frac{1}{(k_2^2+m_{2j}^2)} \prod_{l=1}^{n_3} \frac{1}{((k_1+k_2)^2+m_{3l}^2)} \ .$$

UV and IR singularities are dealt with by dimensional regularization [13] and cancel in the observable quantities. All these integrals can be reduced to one master integral $(m,\, m|m_1|m_2)$ by using partial fraction decomposition, by differentiation and by integration by parts [12, 14]. In particular, by partial fraction decomposition propagators with the same momentum but different masses trivially reduce to integrals of the form (see Fig. 7)

$$V_B(j_1,j_2,j_3,m_1,m_2,m_3) = \int \frac{d^nk_1 d^nk_2}{(k_1^2+m_1^2)^{j_1}(k_2^2+m_2^2)^{j_2}((k_1+k_2)^2+m_3^2)^{j_3}} \tag{24}$$

which in the Appendix are also denoted by $(j_1\ m_1|j_2\ m_2|j_3\ m_3)$. Explicitly the reduction to standard integrals is performed by the following recursion relations obtained by the method of integration by parts [12, 14]:

$$V_B = \frac{\mathbf{1}^-}{2(j_1-1)m_1^2}\left\{j_3\left[\mathbf{1}^- - \mathbf{2}^- - (m_1^2-m_2^2+m_3^2)\right]\mathbf{3}^+ \right.$$
$$\left. + \ (2(j_1-1)+j_3-d)\right\} V_B$$

$$
\begin{aligned}
V_B &= \frac{\Delta(m_1,m_2,m_3)}{j_2-1}\Big\{2j_3m_3^2\,\mathbf{2}^-\left(\mathbf{2}^- - \mathbf{1}^-\right)\mathbf{3}^+ \\
&+ (j_2-1)(m_1^2-m_2^2-m_3^2)\left(\mathbf{3}^- - \mathbf{1}^-\right) \\
&+ \left[2(j_2-1)m_3^2 + 2j_3(m_1^2-m_2^2) + (j_2-1-d)(m_1^2-m_2^2+m_3^2)\right]\mathbf{2}^-\Big\}\,V_B \\
V_B &= \frac{\Delta(m_1,m_2,m_3)}{j_3-1}\Big\{2j_1m_1^2\,\mathbf{1}^+\left(\mathbf{3}^- - \mathbf{2}^-\right)\mathbf{3}^- \\
&+ (j_3-1)(m_1^2-m_2^2+m_3^2)\left(\mathbf{2}^- - \mathbf{1}^-\right) \\
&+ \left[2(j_3-1)m_1^2 + 2j_1(m_2^2-m_3^2) + (j_3-1-d)(m_1^2+m_2^2-m_3^2)\right]\mathbf{3}^-\Big\}\,V_B,
\end{aligned}
\tag{25}
$$

where $\mathbf{1}^{\pm}V_B(j_1,\ldots,m_1,\ldots) \equiv V_B(j_1\pm1,\ldots,m_1,\ldots)$ etc. and

$$
\Delta(m_1,m_2,m_3) = \frac{1}{2m_1^2m_2^2+2m_1^2m_3^2+2m_2^2m_3^2-m_1^4-m_2^4-m_3^4}\quad . \tag{26}
$$

The idea of their application is to reduce all integrals to the master integral

$$
V_B(1,1,1,m_1,m_2,m_3) \tag{27}
$$

and some simple tadpole-integrals, which are obtained when one of the indices is zero. In a first step the integrals with positive index j_1 are reduced to the ones with their first index 1 plus tadpoles. For this purpose the first relation is sufficient even if the index j_3 increases. By inspection one observes that applying all three recursion relations one after the other, the first index does not increase and the sum of all indices decreases by at least 2 (by 1 in each of the last two steps). In this manner j_2 or j_3 must get zero and the procedure can be stopped. Further details and explicit formulae for the master integral and other related two–loop integrals are given in the Appendix.

4. Ward-Takahashi identities, Renormalization

1. Ward-Takahashi identities

We have calculated directly the Z and W self–energies and the $Zb\bar{b}$–vertex in the limit $M_W,\ M_Z \ll m_t$ and m_H arbitrary which is of interest here. Another more elegant approach was used in Ref. [8]. In the limit under consideration S-matrix elements are dominated by the longitudinal vector boson degrees of freedom and according to the *equivalence theorem* [15], with m_t as a high energy scale, one is allowed to replace (up to a phase and up to $O(M/m_t)$ corrections) a longitudinally polarized vector boson by its corresponding unphysical scalar. An equivalent relationship is obtained in the limit of vanishing gauge couplings, g', $g \to 0$, from the Ward-Takahashi identity which derives from the remaining global symmetry [8].

By virtue of these Ward-Takahashi identities for the ρ–parameter we may replace Eq. (2) by

$$\Delta\rho \simeq \Pi'_{\varphi^\pm}(0) - \Pi'_{\varphi}(0) \tag{28}$$

where we have decomposed the Higgs ghost self energies as $\Pi_\varphi(q^2) = \Pi_\varphi(0) + q^2\Pi'_\varphi(q^2)$. This latter expression is simpler to calculate because the scalar vertices are simpler and the number of diagrams to be considered is reduced by roughly a factor of two. The diagrams are depicted in Fig. 5.

The relevant Ward-Takahashi identities derive from the standard model Slavnov-Taylor identities as follows: We use the notation of Ref. [16]. In the 't Hooft gauge we denote by ξ the gauge parameter, ζ and $\eta^\pm$ are the neutral and charged Faddeev–Popov ghost fields, respectively. The Z boson propagator satisfies

$$\begin{aligned} & < T\partial_\mu Z^\mu(x) Z_\nu(y) > + \xi M_Z < T\varphi(x) Z_\nu(y) > \\ = \; & -\xi < T\bar{\zeta}(x)\partial_\nu\zeta(y) > + ig \cos\Theta_W \, \xi < T\bar{\zeta}(x)(W^-_\mu\eta^+ - W^+_\mu\eta^-)(y) > \end{aligned}$$

and

$$\begin{aligned} & < T\partial_\mu Z^\mu(x)\partial_\nu Z^\nu(y) > + \xi M_Z < T\partial_\mu Z^\mu(x)\varphi(y) > \\ & + \xi M_Z < T\varphi(x)\partial_\nu Z^\nu(y) > + \xi^2 M_Z^2 < T\varphi(x)\varphi(y) > = -i\xi\delta(x-y) \end{aligned}$$

for the longitudinal parts of the gauge field propagators. Using the usual tensor decomposition for the self-energy functions (inverse propagators) in Fourier space

$$\begin{array}{rcccl} < TZ^\mu(x)Z^\nu(y) > & \to & iM_Z^2 & (g^{\mu\nu}A_1 + q^\mu q^\nu A_2) & \equiv \; -i\left(g^{\mu\nu}\Pi_Z(q^2) + q^\mu q^\nu \tilde{\Pi}_Z(q^2)\right) \\ < TZ^\mu(x)\varphi(y) > & \to & M_Z & p^\mu B_1 & \\ < T\varphi(x)\varphi(y) > & \to & i & C_1 & \equiv \; i\;\Pi_\varphi(q^2) \\ < T\bar{\zeta}(x)\zeta(y) > + \cdots & \to & -iM_Z^2 & D_1 & \end{array}$$

the above identities read:

$$\begin{aligned} \xi\;(A_1 + q^2A_2 + \;\; B_1) + D_1 &= 0 \\ q^2\;(A_1 + q^2A_2 + 2B_1) + C_1 &= 0 \quad . \end{aligned}$$

By D_1 we have denoted the full Faddeev–Popov ghost contribution which includes both terms of the r.h.s of the first of the above Slavnov-Taylor identities .

In the limit $g \to 0$ the Faddeev-Popov ghosts do not contribute and therefore $D_1 \simeq 0$ such that $A_1 + q^2A_2 + B_1 \simeq 0$. Since the self–energy amplitude A_2 does not exhibit a pole at $q^2 = 0$ we have $q^2A_2 \to 0$. Thus we obtain the relevant Ward-Takahashi identity $A_1 \simeq \frac{C_1}{q^2}$ which we may write in the form

$$\frac{\Pi_Z(q^2)}{M_Z^2} \simeq -\frac{\Pi_\varphi(q^2)}{q^2} = -\Pi'_\varphi(q^2) \tag{29}$$

and which expresses the physical transversal part of the Z self–energy in terms of the self–energy of neutral scalar Higgs ghost. A corresponding relation holds for the W–propagator and this establishes Eq. (28).

For the $Zb\bar{b}$ vertex we have the Slavnov-Taylor identity

$$\begin{aligned} & < T\partial_\mu Z^\mu(x)\psi(y_1)\bar{\psi}(y_2) > + \xi M_Z < T\varphi(x)\psi(y_1)\bar{\psi}(y_2) > \\ = \; & -\xi < T\bar{\zeta}(x) D_{\psi B}\eta_B(y_1)\bar{\psi}(y_2) > - \xi < T\bar{\zeta}(x)\psi(y_1) D_{\bar{\psi}B}\eta_B(y_2) > \end{aligned}$$

where the terms on the right hand side have a fermi field replaced by a composite operator, which are the Becchi-Rouet-Stora (BRS)-variations of the fermi fields ψ and $\bar{\psi}$. In any case these terms do not contribute for on–mass–shell fermions since they do not exhibit the two one particle poles present for the other contributions. Using the following tensor decomposition for the vertex functions (external b–lines amputated and on-shell) in momentum space

$$\begin{aligned} < TZ^\mu(x) b(y_1)\bar{b}(y_2) > \; & \to \; -i\,\tfrac{M_Z}{2v} \;\; (\gamma^\mu(2v_b + F_V) + \gamma^\mu\gamma_5(1 + F_A) + \cdots) \\ < T\varphi(x) b(y_1)\bar{b}(y_2) > \; & \to \; \tfrac{m_b}{v} \;\; (G_S + \gamma_5(1 + G_P) + \cdots) \;\; , \end{aligned} \tag{30}$$

and taking the on–shell matrix element with respect to the external fermions, the above identities read:

$$F_A - G_P - \frac{\delta m_b}{m_b} + 2v_b z_b - \left(A_1 + q^2 A_2 + B_1\right) = 0$$

where the last term in parenthesis is the Z boson propagator contribution which vanishes in the limit $g \to 0$ of interest here. We have denoted by F_i and G_i the nontrivial parts of the amplitudes. They are normalized relative to the axial and pseudoscalar Born terms, respectively. $v_b = \frac{2}{3}\sin^2\Theta_W - \frac{1}{2}$ is the Born level vector coupling. Furthermore we denoted by z_b the axial part of the b wave-function renormalization $\delta Z_b = Z_b - 1 = z_a + \gamma_5 z_b$.

Thus we have

$$F_A = G_P + \frac{\delta m_b}{m_b} - 2v_b z_b \;\; . \tag{31}$$

Instead of discussing the limit $m_b \to 0$ of this identity we may consider directly the case $m_b = 0$. For $m_b = 0$ we actually cannot consider the on-shell matrix element of the ST-identity, because, as $\bar{u}(p')\,(\not{q}, \not{q}\gamma_5)\,u(p) = (0, 2m_b)$ for $q = p' - p$, we do not get a nontrivial relation between the amplitudes. We thus directly compare the off-shell amplitudes proportional to $\not{q}$ and obtain, in agreement with Ref. [8],

$$F_A = G'_P - 2\,(v_b + a_b)\,z_b = G'_P + 2\,(1 - \frac{2}{3}\sin^2\Theta_W)\,z_b \;\; . \tag{32}$$

The amplitudes G'_i are defined now by

$$< T\varphi(x) b(y_1)\bar{b}(y_2) > \to \frac{\not{q}}{2v}\,(G'_S + \gamma_5 G'_P + \cdots) \;\; . \tag{33}$$

Note that the $\varphi b\bar{b}$–vertex has a vanishing Born term in this limit and hence the b wave function renormalization associated with this vertex does not contribute. This causes the change of the coefficient of z_b in Eq. (32).

The amplitudes F_V and G'_S are fixed by the fact that the heavy top effects require a charged current transition and hence must be proportional to $1 - \gamma_5$. Again we see that the calculation

can be simplified considerably because we only need to calculate the simpler diagrams shown in Fig. 6.

However, since we are using computer algebra [17] to evaluate the diagrams it is not too much additional work to calculate directly the amplitudes for the physical fields. The check of the Ward-Takahashi identities provides a welcome test of our calculation. In particular one has a direct check that using an anticommuting γ_5 preserves the Ward-Takahashi identities . More complete calculations which take into account vector boson mass effects (finite g, g') in any case would require to calculate directly the physical amplitudes.

2. Renormalization

Next we must take into account the appropriate counterterms. Since tadpole terms drop out from renormalized quantities in any case we will not include them in any of the bare quantities given in this paper[1]. We first consider the ρ–parameter. Since $\Delta\rho$ is finite at one–loop, as a result of the custodial symmetry of the minimal SM which implies $\rho = 1$ at the tree level, renormalization is simple at the two–loop level. In the approximation we are considering the only renormalization is due to the replacement of the bare top mass by the renormalized one

$$m_{t\,B} = m_t\,(1 + \frac{\delta m_t}{m_t}) \ .$$

By m_t we denote the on–shell mass of the top. Because m_t^2 for the first time shows up as a correction at one–loop order we need the top mass counter term to one–loop order only.

Because the one–loop mass counterterm has a $1/\varepsilon$ singularity for $\varepsilon \to 0$ we have to know the one–loop result which multiplies $\frac{\delta m_t}{m_t}$ to order $O(\varepsilon)$. It was denoted by $\rho^{(1)}$ in Eq. (5) and is given by $\rho^{(1)} = 1 - \varepsilon/2$. In this way we obtain $\rho_{CT}^{(2)}$ as a contribution from the counterterms

$$2\left(1 - \frac{\varepsilon}{2}\right)\frac{\delta m_t}{m_t} = x_t\,\rho_{CT}^{(2)} \ , \tag{34}$$

where x_t was defined in Eq. (5) and δm_t is

$$\frac{\delta m_t^{(1)}}{m_t} = \ x_t\left(\frac{3}{2\varepsilon} + 4 - \frac{a}{2} + \frac{1}{4}a\,(a-6)\ln a + \frac{1}{4}(a-4)\sqrt{a}g(a)\right) \tag{35}$$

calculated from the diagrams of Fig. 8. The result was given in Eq. (11) before.

For the $Zf\bar{f}$–vertex the required counterterms are obtained by replacing bare by renormalized parameters and by the multiplicative field renormalizations (factor $\sqrt{Z_i}$ for each external amputated field). Thus taking into account the radiative corrections amounts to the simple substitution

$$\begin{gathered}\tfrac{M_Z}{v}\gamma^\mu\,(T_{3f}(1-\gamma_5) - 2Q_f s_W^2) \\ \downarrow \\ \tfrac{M_Z}{v}\gamma^\mu\left(T_{3f}(1-\gamma_5)(1+F_A) - 2Q_f s_W^2(1+\tfrac{\delta s_W^2}{s_W^2})\right)\cdot\sqrt{Z_Z}\,Z_f\,\sqrt{1+\tfrac{\delta M_Z^2}{M_Z^2}}\,\sqrt{1+\tfrac{\delta G_\mu}{G_\mu}}\end{gathered} \tag{36}$$

[1]Note that we would have to include tadpole terms if we would insists to work with gauge-invariant counterterms for masses and couplings (see e.g. [18]).

with $s_W^2 = \sin^2\Theta_W$ and we have used $\frac{1}{v^2} = \sqrt{2}G_\mu$. Here, F_A and the counterterms are still functions of the bare parameters which must be replaced by the renormalized one's plus the corresponding counterterms.

Now, for the light fermion vertices $Zf\bar{f}$ $f \neq b,t$ there are no top contributions besides the universal one's entering via the gauge boson self–energies. The corresponding contributions which are incorporated in ρ and κ are finite and gauge invariant by themselves and we need care here only of the additional flavor specific contributions, the vertex and fermion wave-function renormalization corrections. Both corrections are proportional to $1-\gamma_5$. Besides F_A which we directly obtain from the diagrams of Figs. 3a and b we have to calculate Z_b to two-loop order. The irreducible two–loop diagrams which must be calculated are shown in Fig. 9.

The b wave-function renormalization factor is determined as usual by the residuum of the pole of the fermion propagator

$$\tilde{S}_F(p) \;=\; \tfrac{1}{\not p - m_b - \Sigma(p)} \;\to\; Z_b \tfrac{1}{\not p - m_b} \quad \text{for} \quad \not p \to m_b$$

in the limit $m_b \to 0$ we have $\Sigma(p) = \not p \Sigma'(p^2)$ and hence

$$= \tfrac{1}{\not p(1-\Sigma'(p^2))} \;\to\; \tfrac{1}{1-\Sigma'(0)}\tfrac{1}{\not p} \quad \text{for} \quad p^2 \to 0 \quad .$$

Thus

$$Z_b = \frac{1}{1-\Sigma'(0)} \tag{37}$$

and since the leading $m_t \to \infty$ terms are left–handed we have

$$\Sigma'(0) = -(1-\gamma_5)\, z_b \tag{38}$$

in the notation introduced in the previous subsection. If we expand to second order we have

$$Z_b \simeq 1 - (1-\gamma_5)\,[z_b^{(1)} + z_b^{(2)} - 2\,(z_b^{(1)})^2] + \cdots \tag{39}$$

which multiplies the bare vertex from the right. Expanding up to two-loop we obtain (see Eqs. (16,36))

$$\frac{2}{3}s_W^2 \;-\; \frac{1-\gamma_5}{2}\left(1 + F_A^{(1)} - \,2(1-\frac{2}{3}s_W^2)\, z_b^{(1)} + F_A^{(2)} - \,2(1-\frac{2}{3}s_W^2)\,(z_b^{(2)} - 2\,(z_b^{(1)})^2) - 2z_b^{(1)}F_A^{(1)} + \cdots\right)$$

and hence

$$-2x_t^2\tau_b^{(2)} = F_A^{(2)} - \,2(1-\frac{2}{3}s_W^2)\,(z_b^{(2)} - 2\,(z_b^{(1)})^2) - 2z_b^{(1)}F_A^{(1)} \quad . \tag{40}$$

In the following we denote individual contributions by

$$\begin{aligned} -2x_t^2\tau_{Zb\bar{b}}^{(2)} &= F_A^{(2)} \\ -2x_t^2\tau_{b\bar{b}}^{(2)} &= -(1-\frac{2}{3}s_W^2)\, z_b^{(2)} \end{aligned}$$

and

$$\tau_B^{(2)} = \tau_{Zb\bar{b}}^{(2)} + 2\tau_{b\bar{b}}^{(2)} \quad . \tag{41}$$

We finally have to add the contribution from all the remaining counterterms. Besides the remaining b wave function renormalization terms of Eq. (40) we have to include the two–loop effects obtained by replacing to one-loop order the bare parameters m_{tB} and $G_{\mu B}$ in x_t by the renormalized ones in the one-loop result. The bare regularized one-loop result is given by

$$-2x_{tB} = -2x_t\,(1+\varepsilon)\,(m_{tB}/m_t)^{2(1-\epsilon)}\;(1+\frac{\delta G_\mu}{G_\mu})\;. \tag{42}$$

Because the one–loop counterterms have a $1/\varepsilon$ singularity we have to know the one–loop result which multiplies them to order $O(\varepsilon)$ for $\varepsilon \to 0$. In this approximation $\tau_b^{(1)}$ defined in Eq. (18) is given by $\tau_b^{(1)} = 1+\varepsilon$. In the approximation we consider the one-loop result depends on the mass $m_{\varphi^\pm}$ of the charged ghost field $\varphi^\pm$ (see Fig. 3a). The mass counterterm of this field is proportional to

$$\delta m^2_{\varphi^\pm} \propto m_t^2 x_t$$

and we thus have to take into account a term

$$\frac{\partial}{\partial m^2_{\varphi^\pm}}\left(F_A^{(1)} - 2(1-\frac{2}{3}s_W^2)z_b^{(1)}\right)\Big|_{m^2_{\varphi^\pm}=0}\;\delta m^{2(1)}_{\varphi^\pm}\;,$$

which does not vanish in the limit $m^2_{\varphi^\pm} \to 0$. Note that this prescription precisely generates the $\varphi^\pm$ self-energy conterterms needed to renormalize the $\varphi^\pm$ self-energy insertions appearing in the two–loop diagrams of Fig. 3.

Expanding Eq. (36) and using the fact that $Z_Z^{(1)} - 1 + \frac{\delta M_Z^{2(1)}}{M_Z^2} + \frac{\delta G_\mu^{(1)}}{G_\mu}$ is vanishing in the approximation we consider, we obtain $\tau_{CT}^{(2)}$ as a contribution

$$\begin{aligned} -2x_t^2\tau_{CT}^{(2)} &= -2x_t(1+\varepsilon)\left(\frac{\delta G_\mu^{(1)}}{G_\mu} + 2(1-\varepsilon)\frac{\delta m_t^{(1)}}{m_t} - 2z_b^{(1)}\right) \\ &\quad -2x_t\left(\frac{1}{\varepsilon}+2+2\varepsilon+\frac{1}{2}\varepsilon\zeta(2)\right)\frac{\delta m^{2(1)}_{\varphi^\pm}}{m_t^2} \end{aligned} \tag{43}$$

with

$$\begin{aligned} \frac{\delta G_\mu}{G_\mu}^{(1)} &= x_t\left(\frac{a}{2} + 2N_c\,(\frac{1}{\varepsilon}+\frac{1}{2})\right) \\ z_b^{(1)} &= x_t\left(\frac{1}{2\varepsilon}+\frac{3}{4}\right) \end{aligned} \tag{44}$$

and $\frac{\delta m_t}{m_t}$ given by Eq. (35). For the renormalization of the mass of the φ field we find

$$\begin{aligned} \frac{\delta m^{2(1)}_{\varphi^\pm}}{m_t^2} &= -4N_c\left(\frac{1}{\varepsilon}+1+\varepsilon+\frac{1}{2}\varepsilon\zeta(2)\right)x_t \\ &\quad +a^2\left(\frac{1}{\varepsilon}+1+\varepsilon-\ln a+\frac{1}{2}\varepsilon\zeta(2)-\varepsilon\ln a+\frac{\varepsilon}{2}\ln^2 a\right)x_t\;. \end{aligned} \tag{45}$$

Inserting all contributions into Eq. (43) we find

$$\tau_{CT}^{(2)} = -N_c\left(\frac{4}{\varepsilon^2}+\frac{10}{\varepsilon}+17+4\zeta(2)\right)+\frac{a^2}{\varepsilon^2}+(3a^2+2)\frac{1}{\varepsilon}+\frac{11}{2}-\frac{1}{2}a+5a^2+a^2\zeta(2)$$

$$+\frac{1}{2}a^2\ln^2 a-(\frac{a}{\varepsilon}+3+\frac{5}{2}a)a\ln a+(\frac{a}{2}-2)\sqrt{a}g(a). \tag{46}$$

The final result Eq. (20) is then given by

$$\tau_b^{(2)} = \tau_B^{(2)}+\tau_{CT}^{(2)}\ . \tag{47}$$

5. Individual contributions

In this section we present in detail the results for the different amplitudes. Results for individual diagrams are all of a similar form, namely linear combinations of the same basic functions. As the number of diagrams is quite large, especially when working directly with the physical fields, we refrain from giving results for all the individual diagrams. However, results are given for various groups of diagrams.

1. Two-loop heavy top corrections to the ρ parameter:

We first present the bare two–loop corrections for the Z and W propagators. The contribution of $\Pi_V(0)/M_V^2$ to $\rho^{(2)}$, defined in Eq. (5), is denoted by $\rho_V^{(2)}$ such that $\rho_B^{(2)} = \rho_Z^{(2)} - \rho_W^{(2)}$. We obtain the simple results:

$$\rho_Z^{(2)} = -\frac{2a-3}{\varepsilon^2}-\frac{1}{\varepsilon}\left(3a+\frac{43}{2}+4(2-a)\ln a\right)-2(a-2)\ln^2 a+2(3a+2)\ln a$$

$$-\frac{187}{4}-\frac{9}{2}a-(2a-5)\zeta(2)+2\frac{(2a^2-7a+8)}{a}f(a,1)\ , \tag{48}$$

$$\rho_W^{(2)} = -\frac{2a-3}{\varepsilon^2}-\frac{1}{\varepsilon}\left(3a+\frac{37}{2}+4(2-a)\ln a\right)-2(a-2)\ln^2 a+(9a+10)\ln a$$

$$-\frac{261}{4}-\frac{3}{2}a-2\frac{(a^2-a-3)}{a}\zeta(2)$$

$$-\frac{1}{a}(a-4)(3a^2-10a+4)f(a,1)+\frac{3}{a}(a-1)^2(a-2)f(a,0)\ . \tag{49}$$

The functions $f(a,b)$ are defined in Eqs. (6) and (7) and $\zeta(2)=\frac{\pi^2}{6}$.

For the ρ–parameter the results for the different groups of diagrams of Figs. 1a and b are given by

$$\rho_B^{(2,a)} = -C(1+4C)\left[\frac{8}{\varepsilon^2}a+\frac{12}{\varepsilon}a+22a+8a\zeta(2)-\left(\frac{16}{\varepsilon}a+16+24a\right)\ln a\right.$$

$$
\begin{aligned}
&+8a\ln^2 a + \frac{16}{a}\left(2+2a-a^2\right) f(a,1)\Big] \\
&-C^2\left(\frac{96}{\varepsilon}+240\right) + C\left(\frac{4}{\varepsilon^2}-\frac{30}{\varepsilon}-79+12\zeta(2)\right) \\
&+\frac{1}{\varepsilon^2}-\frac{3}{2\varepsilon}-\frac{19}{4}-\zeta(2)-2\ln a+\frac{4+2a}{a}f(a,1)\,, \\
\rho_B^{(2,b)} &= C(1+4C)\Big[\frac{8}{\varepsilon^2}a+\frac{12}{\varepsilon}a+22a+8a\zeta(2)-\left(\frac{16}{\varepsilon}a+16+24a\right)\ln a \\
&+8a\ln^2 a+\frac{16}{a}(2+2a-a^2)f(a,1)\Big] \\
&+C^2\left(\frac{168}{\varepsilon}+420\right)+C\left(\frac{8}{\varepsilon^2}+\frac{48}{\varepsilon}+112+24\zeta(2)\right) \\
&+\frac{2}{\varepsilon^2}-\frac{7}{2\varepsilon}-\frac{19}{4}-a+7\zeta(2)+(2-a)\ln a \\
&-(1-a)^2 f(a,0)-\frac{1}{a}(4-4a+4a^2-a^3)f(a,1)\,, \\
\rho_B^{(2,c)} &= C^2\left(\frac{72}{\varepsilon}+180\right)+C\left(\frac{12}{\varepsilon}+30\right)-\frac{3}{2\varepsilon}-\frac{7}{4}+\frac{4a-2}{a}\zeta(2)-2\ln a \\
&+\frac{2}{a}(1-a)^2 f(a,0)+(8-2a)f(a,1)\,, \\
\rho_B^{(2,d)} &= -C^2\left(\frac{144}{\varepsilon}+360\right)-C\left(\frac{12}{\varepsilon^2}+\frac{30}{\varepsilon}+63+36\zeta(2)\right) \\
&-\frac{3}{\varepsilon^2}+\frac{7}{2\varepsilon}+\frac{119}{4}-2a-\frac{4+7a}{a}\zeta(2)-(4+2a)\ln a \\
&+\frac{2}{a}(2-a)(1-a)^2 f(a,0)+2(a-2)(a-4)f(a,1)\ . \qquad (50)
\end{aligned}
$$

The sum of these contributions yields Eq. (10). The constant C, which drops out from the sum of the above contributions, is the vector coupling coefficient of the $Zt\bar{t}$ vertex, $C = -2/3\sin^2\Theta_W + 1/4$.

If we make use of the Ward-Takahashi identity we have to calculate the neutral and charged Higgs ghost field propagators as has been done in Ref. [8]. The two-loop contributions increasing proportional to m_t^2 and m_t^4 are due to the diagrams depicted in Fig. 5 where we have grouped the diagrams as in Ref. [8] to allow for a direct comparison.

In terms of the functions Eqs. (6) and (7) the unrenormalized contributions from different groups of diagrams read

$$
\rho_B^{(2,a)} = -2+\frac{2\,(6-a)}{a-4}\ln a-\frac{4\,(a^2-6a+6)}{a(a-4)}\,f(a,1),
$$

$$\rho_B^{(2,b)} = -\frac{3}{\varepsilon} + \frac{29}{2} - 3a + (4 - 3a + \frac{4}{a-4})\ \ln a - \frac{5}{6}\pi^2$$
$$- (3a^2 - 12a + 7)\ f(a,0) + \left(3a^2 - 18a + 26 - \frac{6}{a} + \frac{2}{a-4}\right) f(a,1),$$
$$\rho_B^{(2,c)} = 6 + \frac{2a-3}{3a}\ \pi^2 + \frac{4\,(6-a)}{a-4}\ \ln a + \frac{6-4a}{a}\ f(a,0) + \frac{4\,(a-3)}{a-4}\ f(a,1),$$
$$\rho_B^{(2,d)} = -\frac{4a}{a-4}\ \ln a + \frac{2\pi^2}{3} - 4f(a,0) + \frac{4\,(a-6)}{a-4} f(a,1)\ . \qquad (51)$$

A comparison of the results Eq. (50) with (51) shows that the use of the Ward-Takahashi identity leads to noticeable simplification of the expressions. The sums of the contributions agree as they should.

2. Two-loop heavy top corrections to the τ parameter:

The two–loop corrections to the $Zb\bar{b}$ vertex may be expressed in terms of the τ parameter which was defined in Eq. (18). We distinguish two groups of unrenormalized diagrams:

a) Contribution from diagrams without Higgs and neutral Goldstone particles shown in Fig. 3a. The result is

$$\tau_{Zb\bar{b}}^{(2,a)} = 2N_c\left[C\left(\frac{7}{\varepsilon^2} + \frac{31}{2\varepsilon} + \frac{111}{4} + 9\zeta(2)\right) + \frac{9}{4\varepsilon^2} + \frac{49}{8\varepsilon} + \frac{161}{16} + \frac{7}{4}\zeta(2)\right]$$
$$-C\left(\frac{1}{\varepsilon^2} + \frac{3}{2\varepsilon} + \frac{7}{4} + 3\zeta(2)\right) + \frac{1}{4\varepsilon^2} - \frac{13}{8\varepsilon} - \frac{25}{16} + \frac{3}{4}\zeta(2)\ . \qquad (52)$$

b) Contribution from diagrams with Higgs and neutral Goldstone particles shown in Fig. 3b. Here the result reads

$$\tau_{Zb\bar{b}}^{(2,b)} = -4C\sigma + C\left(\frac{1}{\varepsilon^2} + \frac{3}{2\varepsilon} + \frac{7}{4} + 3\zeta(2)\right) - \frac{4a^2-1}{4\varepsilon^2} - \left(\frac{17}{8} + \frac{7}{2}a^2 - a^2\ln a\right)\frac{1}{\varepsilon}$$
$$+\frac{99}{16} - \frac{17}{4}a - \frac{33}{4}a^2 - (\frac{1}{2} + 5a^2 - 4a^3)\zeta(2) - (\frac{11}{4} - a)a\ln a - (\frac{5}{2} - 2a)a^2\ln^2 a$$
$$-\frac{1}{4}(a-1)^2(7-22a)f(a,0) + \left(8 - \frac{47}{2}a + \frac{47}{4}a^2 - \frac{3}{2}a^3\right) f(a,1)\ . \qquad (53)$$

The contribution to the τ parameter from the unrenormalized $Zb\bar{b}$ vertex is given by the sum of these two terms:

$$\tau_{Zb\bar{b}}^{(2)} = 2N_c\left[C\left(\frac{7}{\varepsilon^2} + \frac{31}{2\varepsilon} + \frac{111}{4} + 9\zeta(2)\right) + \frac{9}{4\varepsilon^2} + \frac{49}{8\varepsilon} + \frac{161}{16} + \frac{7}{4}\zeta(2)\right]$$
$$-4C\sigma - \frac{2a^2-1}{2\varepsilon^2} - \left(\frac{15}{4} + \frac{7}{2}a^2 - a^2\ln a\right)\frac{1}{\varepsilon} + \frac{37}{8} - \frac{17}{4}a - \frac{33}{4}a^2$$

$$+(\frac{1}{4}-5a^2+4a^3)\zeta(2)-(\frac{11}{4}-a)a\ln a-(\frac{5}{2}-2a)a^2\ln^2 a$$

$$-\frac{1}{4}(a-1)^2(7-22a)f(a,0)+\left(8-\frac{47}{2}a+\frac{47}{4}a^2-\frac{3}{2}a^3\right)f(a,1)\ . \qquad (54)$$

For the renormalization of the $Zb\bar{b}$ vertex we need the b wave-function renormalization factor. To this end we have to calculate the two-loop corrections to the b–propagator. The diagrams are given in Fig. 9.

The unrenormalized expression for the b propagator is

$$\tau_{b\bar{b}}^{(2)} \ = \ -(2C-\frac{1}{2})\left[N_c\left(\frac{7}{2\varepsilon^2}+\frac{31}{4\varepsilon}+\frac{111}{8}+\frac{9}{2}\zeta(2)\right)-\sigma\right] \qquad (55)$$

with the shorthand

$$\begin{aligned}\sigma \ &= \ \frac{2a^2+1}{2\varepsilon^2}+\frac{10a^2+1}{4\varepsilon}-\frac{19}{8}+\frac{5}{4}a+\frac{23}{4}a^2+(\frac{3}{4}+4a^2-2a^3)\zeta(2)\\ &+(-\frac{a}{\varepsilon}+\frac{3}{4}-a)a\ln a+(2-a)a^2\ \ln^2 a\\ &+(a-1)^2\frac{7-10a}{4}f(a,0)+\frac{2a^2-11a+6}{4}\ (a-4)\ f(a,1)\ . \qquad (56)\end{aligned}$$

The contribution from the bare two-loop diagrams to the τ parameter thus is

$$\begin{aligned}\tau_B^{(2)} \ &= \ \tau_{Zb\bar{b}}^{(2)}+2\tau_{b\bar{b}}^{(2)}\\ &= \ 2N_c\left(\frac{2}{\varepsilon^2}+\frac{5}{\varepsilon}+\frac{17}{2}+2\zeta(2)\right)-\frac{a^2}{\varepsilon^2}-\frac{3a^2+2}{\varepsilon}+\frac{7}{2}-\frac{11}{4}a-7a^2\\ &-\frac{1+18a^2-12a^3}{4}\zeta(2)-\frac{9-6a}{4}a^2\ln^2 a+\left(\frac{1}{\varepsilon}a^2-\frac{7}{4}a+a^2\right)\ln a\\ &-(a-1)^2\frac{7-16a}{4}f(a,0)+\left(7-18a+\frac{33}{4}a^2-a^3\right)f(a,1). \qquad (57)\end{aligned}$$

If we make use of the Ward-Takahashi identity, we just have to calculate the $\varphi b\bar{b}$ vertex, where φ is the neutral Higgs ghost field. Such a calculation has been done in Ref. [8]. The two-loop contributions increasing proportional to m_t^2 and m_t^4 are due to the diagrams depicted in Fig. 6. Again, we have grouped the diagrams as in Ref. [8] to allow for a direct comparison.

Again, we use the notation (see Eq. (32))

$$-2x_t^2\tau_{\varphi b\bar{b}}^{(2)}=G_P'^{(2)} \qquad (58)$$

and write

$$\tau_{\varphi b\bar{b}}^{(2)}=-2\delta Z_1 \qquad (59)$$

in terms of Z_1 in order to conform with the notation of [8]. The contributions from different groups of diagrams shown in Fig. 6 are:

$$\begin{aligned}
\delta Z_1^{(a)} &= \frac{a}{8} - \frac{a^2}{8}(2+a)\zeta(2) - \frac{a^2}{16}(2+a)\ln^2 a \\
&+ \frac{a}{4}(1-a-a^2)f(a,0) + \frac{a}{8}(a^2-2a-4)f(a,1), \\
\delta Z_1^{(b)} &= \frac{1}{2}N_c, \\
\delta Z_1^{(c)} &= -\frac{a}{8} + \frac{5}{8}\zeta(2) - \frac{a}{8}\ln a \\
&- \frac{1}{8}(a^2-8a+5)f(a,0) + \frac{1}{8}(a^2-10a+20)f(a,1), \\
\delta Z_1^{(d)} &= \frac{3}{8}a + \frac{3}{8}a^2(4-a)\zeta(2) + \frac{3a^2}{16}(4-a)\ln^2 a \\
&- \frac{a}{4}(7-15a+3a^2)f(a,0) + (\frac{11}{2}a - 3a^2 + \frac{3}{8}a^3)f(a,1), \\
\delta Z_1^{(e)} &= a^2 + (\frac{1}{\varepsilon}+1)N_c + a^2\ln a + \frac{a^2}{4}(1-2a)\ln^2 a \\
&+ \frac{a^2}{2}(1-2a)\zeta(2) + \frac{a^2}{2}(1-2a)f(a,0) \\
\delta Z_1^{(f)} &= \frac{1}{\varepsilon} - \frac{7}{4} + a + (a-\frac{3}{4})\ln a - \frac{1}{4}\zeta(2) \\
&+ (\frac{9}{4} - \frac{7}{2}a + a^2)f(a,0) + (\frac{3}{2a} - \frac{29}{4} + \frac{11}{2}a - a^2)f(a,1), \\
\delta Z_1^{(g)} &= \frac{3}{4}\ln a - \frac{1}{4}\zeta(2) + \frac{1}{4}(a-3)f(a,0) + (-\frac{3}{2a} + \frac{5}{4} - \frac{1}{4}a)f(a,1). \qquad (60)
\end{aligned}$$

Here for the diagrams of group (e), the counterterms corresponding to the mass of the φ field are taken into account. For all other diagrams we give the unrenormalized expressions. For the sum of the above diagrams we then have

$$\begin{aligned}
\delta Z_1 &= \frac{1}{\varepsilon} - \frac{7}{4} + \frac{11}{8}a + a^2 + (\frac{1}{8} + \frac{7}{4}a^2 - \frac{3}{2}a^3)\zeta(2) + (\frac{1}{\varepsilon} + \frac{3}{2})N_c \\
&+ \frac{a}{8}(7+8a)\ln a + \frac{a^2}{8}(7-6a)\ln^2 a \qquad (61) \\
&- (a-1)^2(2a-\frac{7}{8})f(a,0) + (\frac{a^3}{2} - \frac{33}{8}a^2 + 9a - \frac{7}{2})f(a,1)\ .
\end{aligned}$$

The counterterms for the $\varphi b\bar{b}$ vertex (see Eq. (33)) follow from

$$(1-\gamma_5)\,G'_P\;(1+(1-\gamma_5)z_b)^{-1} = (1-\gamma_5)\,G'_P\,(1-2z_b+\cdots) \tag{62}$$

and the replacement of bare by renormalized parameters in the one–loop result. Note that the Born term is absent for $m_b = 0$. This naive renormalization prescription, as it should, yields the renormalized physical $Zb\bar{b}$ amplitude F_A^{ren} which is given by

$$F_A^{ren} = ((1-\frac{2}{3}s_W^2)+F_A)/(1+2z_b) - (1-\frac{2}{3}s_W^2) = G'_P/(1+2z_b) \tag{63}$$

where the last equality follows from the WT–identity Eq. (32). Using the bare regularized one-loop result Eq. (42) the analog of Eq. (43) reads

$$-2x_t^2\tilde{\tau}_{CT}^{(2)} = -2x_t\,(1+\varepsilon)\left(\frac{\delta G_\mu^{(1)}}{G_\mu} + 2(1-\varepsilon)\frac{\delta m_t^{(1)}}{m_t} - 2z_b^{(1)}\right) \tag{64}$$

where the relevant quantities have been given in Eqs. (35,44). Note that the contribution from the $\varphi^\pm$ mass counterterm has been subtracted already in Eq. (61). The remaining counterterm contribution is then given by

$$\tilde{\tau}_{CT}^{(2)} = 2N_c\left(\frac{1}{\varepsilon}+\frac{3}{2}\right) + \frac{2}{\varepsilon} + \frac{11}{2} - \frac{a}{2} + \frac{a(a-6)}{2}\ln a + \left(\frac{a}{2}-2\right)\sqrt{a}g(a). \tag{65}$$

Adding these contributions

$$\tau_b^{(2)} = \tau_{\varphi b\bar{b}}^{(2)} + \tilde{\tau}_{CT}^{(2)} \tag{66}$$

we recover our result Eq. (20).

Acknowledgment.

One of us (O.T.) is grateful to the Physics Department of the Bielefeld University for warm hospitality and to BMFT for financial support.

References

1 The LEP Collaboration: ALEPH, DELPHI, L3 and OPAL, Phys. Lett. B276 (1992) 247;
D. Schaile, Talk given at the "27th International Conference on High Energy Physics", Glasgow, July 1994.

2 K. Abe et al., Phys. Rev. Lett. 73 (1994) 25;
M. Fero, Talk given at the "27th International Conference on High Energy Physics", Glasgow, July 1994.

3 C.K. Jung, Talk given at the "27th International Conference on High Energy Physics", Glasgow, July 1994.

4 F. Abe et al., *Evidence for Top Quark Production in $\bar{p}p$ collisions at $\sqrt{s} = 1.8$ TeV*, FERMILAB Pub-94/097-E CDF, April 1994;
H. Jensen, Talk given at the "27th International Conference on High Energy Physics", Glasgow, July 1994; P. Grannis, ibid.

5 M. Veltman, Nucl. Phys. B123 (1977) 89.

6 A. Akhundov, D. Bardin and T. Riemann, Nucl. Phys. B276 (1986) 1;
W. Beenakker and W. Hollik, Z. Phys. C40 (1988) 141;
J. Bernabeu, A. Pich and A. Santamaria, Phys. Lett. B200 (1988) 569.

7 J. Van der Bij and F. Hoogeveen, Nucl. Phys. B 283 (1987) 477.

8 R. Barbieri, M. Beccaria, P. Ciafaloni, G. Curci and A. Viceré,
Phys. Lett. B288 (1992) 95; ibid. B312 (1993) 511 (E); Nucl. Phys. B409 (1993) 105.

9 A. Denner, W. Hollik and B. Lampe, Z. Phys. C60 (1993) 193.

10 J. Fleischer, O.V. Tarasov and F. Jegerlehner, Phys. Lett. B319 (1993) 249.

11 M. Consoli, W. Hollik and F. Jegerlehner, Phys. Lett. B 227 (1989) 167.

12 J. Van der Bij and M. Veltman, Nucl. Phys. B231 (1984) 205.

13 G. t'Hooft, M. Veltman, Nucl.Phys. B44 (1972) 189;
C. G. Bollini, J.J. Giambiagi, Nuovo Cim. 12A (1972) 20.

14 F.V. Tkachov, Phys. Lett. B100 (1981) 65;
K.G. Chetyrkin and F.V. Tkachov, Nucl. Phys. B192 (1981) 159;
F. Hoogeveen, Nucl. Phys. B259 (1985) 19;
A.I. Davydychev and J.B. Tausk, Nucl.Phys. B397 (1993) 123;
J. Fleischer and O.V. Tarasov, Comput. Phys. Commun. 71 (1992) 193.

15 J. M. Cornwall, D. N. Levin and G. Tiktopoulos, Phys. Rev. D10 (1974) 1145;
M. S. Chanowitz and M. K. Gaillard, Nucl. Phys. B261 (1985) 379;
J. Bagger and C. Schmidt, Phys. Rev. D41 (1990) 264;
H. Veltman, Phys. Rev. D41 (1990) 2294;
H.-J. He, Y.-P. Kuang and X. Li, Phys. Rev. Lett. 69 (1992) 2619.

16 F. Jegerlehner, in "Testing the Standard Model",
eds. M. Cvetič, P. Langacker, World Scientific, Singapore, 1991.

17 J.A.M. Vermaseren: Symbolic manipulation with FORM
(Computer Algebra Nederland, Amsterdam, 1991).

18 J. Fleischer and F. Jegerlehner, Phys. Rev. D23 (1981) 2001.

Appendix: Useful Integrals

In this Appendix we discuss properties of the master integrals. The relationships found here were crucial in obtaining simple compact formulae. Using recurrence relations obtained by the integration-by-parts technique [12, 14] all integrals were reduced, with the help of FORM [17], to two integrals, which are special cases of

$$f(a,b) = \int_0^1 dx \left(\mathrm{Sp}\,(1-\mu^2) + \frac{\mu^2}{\mu^2-1} \ln \mu^2 \right) \quad ; \quad \mu^2 = \frac{ax + b\,(1-x)}{x\,(1-x)}$$

given in Ref. [12]. We consider a slightly generalized situation where we have three different masses m, m_H and m' in the problem. We denote the mass ratios by

$$a = \frac{m_H^2}{m^2} \; , \quad b = \frac{m'^2}{m^2} \; .$$

We first define the symmetric auxiliary function

$$\begin{aligned} h(a,b) \;&=\; -\mathrm{Sp}(1-\frac{y_1}{x_1}) - \mathrm{Sp}(1-\frac{x_1}{y_1}) + \mathrm{Sp}(1-\frac{y_2}{x_2}) + \mathrm{Sp}(1-\frac{x_2}{y_2}) \\ &\quad +\mathrm{Sp}\;(-\frac{y_2}{x_1}) \;\; -\mathrm{Sp}\;(-\frac{x_1}{y_2}) - \mathrm{Sp}\;(-\frac{y_1}{x_2}) + \mathrm{Sp}\;(-\frac{x_2}{y_1}) \\ &=\; 2 \;\; \left(\mathrm{Sp}\,(-\frac{x_2}{y_1}) - \mathrm{Sp}\,(-\frac{x_1}{y_2}) \right) \\ &\quad +\frac{1}{2} \left(\ln^2(\frac{x_2}{y_1}) - \ln^2(\frac{x_1}{y_2}) + \ln^2(\frac{x_1}{y_1}) - \ln^2(\frac{x_2}{y_2}) \right) \end{aligned}$$

with

$$\begin{aligned} x_1 &= \frac{1}{2}(1-a+b+\sqrt{\lambda}\,) \; , \quad x_2 = \tfrac{1}{2}(1-a+b-\sqrt{\lambda}\,) \\ y_1 &= \frac{1}{2}(1+a-b+\sqrt{\lambda}\,) \; , \quad y_2 = \tfrac{1}{2}(1+a-b-\sqrt{\lambda}\,) \end{aligned}$$

and

$$\lambda = 1 - 2\,(a+b) + (a-b)^2 \quad .$$

The roots satisfy the simple relationships

$$\begin{aligned} y_1 \;&=\; 1-x_2 \;\; , \quad\;\; y_2 \;=\; 1-x_1 \\ x_1 x_2 \;&=\; \;\; b \;\;\; , \quad y_1 y_2 \;=\; \;\; a \;\;\; . \end{aligned}$$

For $b=1$ we denote $x_1|_{b=1}$ by ξ and have $x_2 = 1/\xi$, $y_1 = 1 - 1/\xi$ and $y_2 = 1-\xi$ where

$$\xi = \frac{\sqrt{1-y}-1}{\sqrt{1-y}+1} \quad ; \quad y = 4a^{-1}$$

takes the values

$$\begin{aligned} 0 \le \xi \le 1 \qquad & \text{for} \quad a \le 0 \\ \xi = e^{i\varphi},\ 0 \le \varphi \le \pi \quad & \text{for} \quad 4 \ge a \ge 0 \\ -1 \le \xi \le 0 \qquad & \text{for} \quad 4 \le a\ . \end{aligned}$$

The function $h(a,1)$ now has the simple form

$$h(a,1) = 2\left[\mathrm{Sp}(1) + 2\,\mathrm{Sp}(\xi) + \frac{1}{2}\ln^2(-\xi)\right] \quad .$$

The function $h(a,1)$ is real for $a \ge 4$ and purely imaginary

$$h(a,1) = i\ 4\ \ C\ell_2(\varphi)$$

when $4 \ge a \ge 0$, with $\varphi = 2\arcsin\sqrt{1/y}$ and $C\ell_2(\varphi) = \mathrm{Im}\ \mathrm{Sp}(e^{i\varphi})$ is the Clausen function.

For $b = a$ we have $y_1 = x_1$, $y_2 = x_2 = 1 - x_1$ and $-x_2/y_1 = -y_2/x_1 = \xi$ is given by the formula above but with the replacement $a \to a^{-1}$. Thus

$$h(a,a) = h(a^{-1},1) \quad .$$

The master integrals may be expressed in terms of the function

$$f(a,b) \ = \ -\frac{1}{2}\left(\ln(a)\ln(b) + \frac{a+b-1}{\sqrt{\lambda}}\ h(a,b)\right)$$

and derivatives of it. For special values of the arguments we obtain:

$$\begin{aligned} f(a,1) \ &= \ -\frac{h(a,1)}{2\sqrt{1-y}} \\ &= \ \begin{cases} -\frac{1}{\sqrt{1-y}}\left[\mathrm{Sp}(1) + 2\,\mathrm{Sp}(\xi) + \frac{1}{2}\ln^2(-\xi)\right] & ;\ a \ge 4 \\ -\frac{2}{\sqrt{y-1}}\ \ C\ell_2(\varphi) & ;\ 4 \ge a \ge 0 \end{cases} \\ f(a,0) \ &= \ \mathrm{Sp}(1-a) \ = \ \mathrm{Sp}(1) - \mathrm{Sp}(a) - \ln(a)\ln(1-a) \\ f(a^{-1},0) \ &= \ -f(a,0) - \frac{1}{2}\ln^2(a) \\ f(a^{-1},a^{-1}) \ &= \ -\frac{1}{2}\ln^2(a) + (\frac{2}{a} - 1)f(a,1) \quad . \end{aligned}$$

For the derivatives we have

$$\begin{aligned} \frac{\partial}{\partial a} f(a,b) \ &= \ \frac{2b}{\lambda}\ln(b) - \frac{a+b-1}{\lambda}\ln(a) + \frac{b\,(a-b+1)}{\lambda^{3/2}}\ h(a,b) \\ &\overset{b\equiv 1}{=} \ \frac{-1}{a-4}\left[\ln(a) + \frac{2}{a}f(a,1)\right] \\ \frac{\partial}{\partial b} f(a,b) \ &= \ \frac{2a}{\lambda}\ln(a) - \frac{a+b-1}{\lambda}\ln(b) - \frac{a\,(a-b-1)}{\lambda^{3/2}}\ h(a,b) \\ &\overset{b\equiv 1}{=} \ \frac{2}{a-4}\left[\ln(a) - (\frac{2}{a} - 1)f(a,1)\right] \end{aligned}$$

$$a\frac{\partial f}{\partial a} + b\frac{\partial f}{\partial b} = \frac{2ab}{\lambda}\ln(ab) - \frac{a+b-1}{\lambda}(a\ln(a)+b\ln(b)) + \frac{2ab}{\lambda^{3/2}}\ h(a,b)$$

$$\stackrel{b=1}{=} \frac{1}{a-4}\left[(2-a)\ln(a) - \frac{4}{a}f(a,1)\right]$$

For $b = 0$ we find

$$\frac{\partial}{\partial a}f(a,b)\Big|_{b=0} = \frac{\ln(a)}{1-a}$$

Special values:

$$f(4,1) = -4\ln(2) \qquad f(1/4,1/4) = 2\ln(2)\,(1-\ln(2))$$

$$\tfrac{\partial f}{\partial a}(4,1) = -\tfrac{1}{6} - \tfrac{1}{3}\ln(2) \qquad \tfrac{\partial f}{\partial b}(4,1) = \tfrac{1}{3} - \tfrac{4}{3}\ln(2)$$

$$f(1,0) = 0 \qquad f(0,0) = \tfrac{\pi^2}{6}$$

$$\tfrac{\partial f}{\partial a}(1,0) = -1 \qquad \tfrac{\partial f}{\partial b}(0,1) = -1$$

The asymptotic expansion of $f(a,1)$ reads:

$$\begin{aligned} f(a,1) = &- \log(a)^2\,(\frac{1}{2} + a^{-1} + 3\,a^{-2} + 10\,a^{-3} + 35\,a^{-4} + \cdots) \\ &+ \log(a)\,(2\,a^{-1} + 7\,a^{-2} + 74/3\,a^{-3} + 533/6\,a^{-4} + \cdots) \\ &- \zeta(2)\,(1 + 2\,a^{-1} + 6\,a^{-2} + 20\,a^{-3} + 70\,a^{-4} + \cdots) \\ &+ 2\,a^{-1} + 11/2\,a^{-2} + 155/9\,a^{-3} + 4163/72\,a^{-4} + \cdots \quad a \to \infty \\ f(a,1) = &\ \log(a)\,(1/2\,a + 1/12\,a^2 + 1/60\,a^3 + 1/280\,a^4 + 1/1260\,a^5 + \cdots) \\ &- (a + 5/36\,a^2 + 47/1800\,a^3 + 319/58800\,a^4 + 1879/1587600\,a^5 + \cdots) \quad a \to 0 \end{aligned}$$

Denoting

$$n = 4 - 2\epsilon \ \text{ and } \ \gamma + \ln\pi + \ln m_i^2 \equiv \ln M_i^2$$

we obtain the following list of integrals which have been used in our calculation:

$$
\begin{aligned}
J_1 \;=\; (3m|m_H|m) \;&=\; -\tfrac{1}{2}\tfrac{\partial}{\partial m^2}(2m|m_H|m')\Big|_{m'=m} \\
&=\; \tfrac{\pi^4}{m^2}\left(-\tfrac{1}{2\epsilon}-\tfrac{1}{2}+\ln(M^2)-\tfrac{1}{2}(a\tfrac{\partial f}{\partial a}+b\tfrac{\partial f}{\partial b})_{b=1}\right) \\
&=\; \tfrac{\pi^4}{m^2}\left(-\tfrac{1}{2\epsilon}-\tfrac{1}{2}+\ln(M^2)-\tfrac{1}{2}\tfrac{1}{a-4}\left[(2-a)\ln a-\tfrac{4}{a}f(a,1)\right]\right)
\end{aligned}
$$

$$
\begin{aligned}
J_2 \;=\; (2m|m_H|2m) \;&=\; -\tfrac{\partial}{\partial m'^2}(2m|m_H|m')\Big|_{m'=m} = \tfrac{\pi^4}{m^2}\tfrac{\partial f(a,b)}{\partial b}\Big|_{b=1} \\
&=\; \tfrac{\pi^4}{m^2}\left(\tfrac{2}{a-4}\left[\ln a-(\tfrac{2}{a}-1)f(a,1)\right]\right)
\end{aligned}
$$

$$
\begin{aligned}
J_3 \;=\; (2m|m_H|m) \;&=\; \pi^4\left(-\tfrac{1}{2\epsilon^2}-\tfrac{1}{2\epsilon}\,(1-2\ln(M^2))\right. \\
&\quad \left.-\tfrac{1}{2}-\tfrac{1}{2}\zeta(2)+\ln(M^2)-\ln^2(M^2)-f(a,1)\right)
\end{aligned}
$$

$$
\begin{aligned}
J_4 \;=\; (m|m_H|m) \;&=\; -2m^2J_3-m_H^2J_9+ \\
&\quad \pi^4\left((\tfrac{1}{\epsilon}+3)\,(2m^2+m_H^2)-2\,(2m^2\ln(M^2)+m_H^2\ln(M_H^2))\right)
\end{aligned}
$$

$$
\begin{aligned}
J_5 \;=\; (2\;0|m_H|m) \;&=\; \pi^4\left(\tfrac{1}{2\epsilon^2}+\tfrac{1}{2\epsilon}\,(1-2\ln(M_H^2))\right. \\
&\quad +\tfrac{1}{2}-\tfrac{11}{2}\zeta(2)-\ln(M_H^2)+\ln^2(M_H^2) \\
&\quad \left.-\tfrac{\ln(a)}{a-1}\,(\tfrac{1}{\epsilon}+1-2\ln(M_H^2)+\tfrac{1}{2}\ln(a)\,)-\tfrac{1+a}{1-a}f(a^{-1},0)\right)
\end{aligned}
$$

$$
\begin{aligned}
J_6 \;=\; (2m|m_H|0) \;&=\; \pi^4\left(-\tfrac{1}{2\epsilon^2}-\tfrac{1}{2\epsilon}\,(1-2\ln(M^2))\right. \\
&\quad \left.-\tfrac{1}{2}-\tfrac{1}{2}\zeta(2)+\ln(M^2)-\ln^2(M^2)-f(a,0)\right)
\end{aligned}
$$

$$
\begin{aligned}
J_7 \;=\; (m|m_H|0) \;&=\; -m^2J_6-m_H^2J_{10}+ \\
&\quad \pi^4\left((\tfrac{1}{\epsilon}+3)\,(m^2+m_H^2)-2\,(m^2\ln(M^2)+m_H^2\ln(M_H^2))\right)
\end{aligned}
$$

$$
\begin{aligned}
J_8 \;=\; (2m|2m_H|m) \;&=\; -\tfrac{\partial}{\partial m_H^2}(2m|m_H|m')\Big|_{m'=m} = \tfrac{\pi^4}{m^2}\tfrac{\partial f(a,b)}{\partial a}\Big|_{b=1} \\
&=\; \tfrac{\pi^4}{m^2}\left(\tfrac{-1}{a-4}\left[\ln a+\tfrac{2}{a}f(a,1)\right]\right)
\end{aligned}
$$

$$
\begin{aligned}
J_9 \;=\; (m|2m_H|m) \;&=\; \pi^4\left(-\tfrac{1}{2\epsilon^2}-\tfrac{1}{2\epsilon}\,(1-2\ln(M_H^2))\right. \\
&\quad \left.-\tfrac{1}{2}-\tfrac{1}{2}\zeta(2)+\ln(M_H^2)-\ln^2(M_H^2)-f(a^{-1},a^{-1})\right)
\end{aligned}
$$

$$
\begin{aligned}
J_{10} \;=\; (m|2m_H|0) \;&=\; \pi^4\left(-\tfrac{1}{2\epsilon^2}-\tfrac{1}{2\epsilon}\,(1-2\ln(M_H^2))\right. \\
&\quad \left.-\tfrac{1}{2}-\tfrac{1}{2}\zeta(2)+\ln(M_H^2)-\ln^2(M_H^2)-f(a^{-1},0)\right)
\end{aligned}
$$

$$
J_{11} \;=\; (2m|2m_H|0) \;=\; -\tfrac{\partial}{\partial m_H^2}(2m|m_H|0) = \tfrac{\pi^4}{m^2}\tfrac{\partial f(a,0)}{\partial a} = \tfrac{\pi^4}{m^2}\tfrac{\ln a}{1-a}
$$

Figure captions

Fig. 1a: Leading 2-loop electroweak diagrams contributing to the Z self-energy. Heavy full lines represent the top, light full lines the bottom quarks; dashed lines stand for the charged "would-be Goldstone bosons" $\varphi^{\pm}$, dotted lines for the neutral Higgs ghost φ and the physical Higgs H.

Fig. 1b: Leading 2-loop electroweak diagrams contributing to the W self-energy. Internal lines have the same meaning as in Fig. 1a.

Fig. 2a: $\rho^{(2)}$ as a function of a compared with the asymptotic expansions for small and large a.

Fig. 2b: $\rho^{(2)}$ as a function of a. The bare contribution $\rho_B^{(2)}$ and the top mass counterterm $\rho_{CT}^{(2)}$, which here is subtracted at $a = 0$, are shown separately. $\rho_{\overline{MS}}^{(2)}$ shows the result obtained when the $\overline{MS}$ definition is adopted for the top quark mass.

Fig. 3a: Leading electroweak loop diagrams without Higgs and neutral Higgs ghosts contributing to the $Zb\bar{b}$ vertex. Internal lines have the same meaning as in Fig. 1.

Fig. 3b: Leading 2-loop electroweak diagrams involving Higgs and neutral Higgs ghosts contributing to the $Zb\bar{b}$ vertex. Notice that φ does not couple to $\varphi^{\pm}$. Internal lines have the same meaning as in Fig. 1.

Fig. 4a: $\tau^{(2)}$ as a function of a compared with the asymptotic expansions for small and large a.

Fig. 4b: $\tau^{(2)}$ as a function of a. The bare contribution $\tau_B^{(2)}$ and the top mass counterterm $\tau_{CT}^{(2)}$, which here is subtracted at $a = 0$, are shown separately. $\tau_{\overline{MS}}^{(2)}$ shows the result for the $\overline{MS}$ definition of the top quark mass.

Fig. 5: Leading 2-loop electroweak diagrams contributing to the φ and $\varphi^{\pm}$ self-energy, labeled as in Ref. [8]. Internal lines have the same meaning as in Fig. 1.

Fig. 6: Leading 2-loop electroweak diagrams contributing to the $\varphi b\bar{b}$ vertex, labeled as in Ref. [8]. Internal lines have the same meaning as in Fig. 1.

Fig. 7: General type of "bubble" diagram obtained in a heavy mass expansions at the two-loop level. In this Figure each line stands for a chain of propagators of equal mass.

Fig. 8: Leading 1-loop corrections to the top propagator. The different lines have the same meaning as in Fig. 1.

Fig. 9: Leading loop corrections to the bottom quark propagator. The different lines have the same meaning as in Fig. 1.

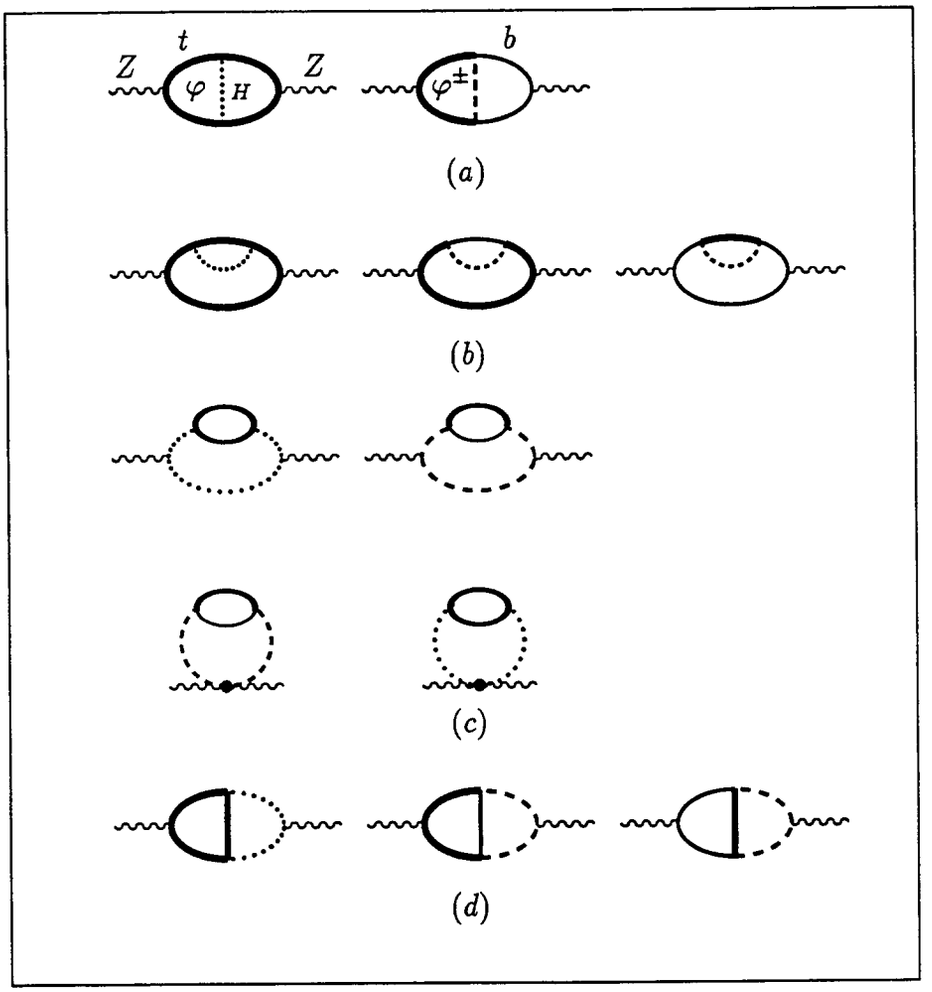

Fig. 1a: Leading 2-loop electroweak diagrams contributing to the Z self-energy. Heavy full lines represent the top, light full lines the bottom quarks; dashed lines stand for the charged "would-be Goldstone bosons" $\varphi^{\pm}$, dotted lines for the neutral Higgs ghost φ and the physical Higgs H.

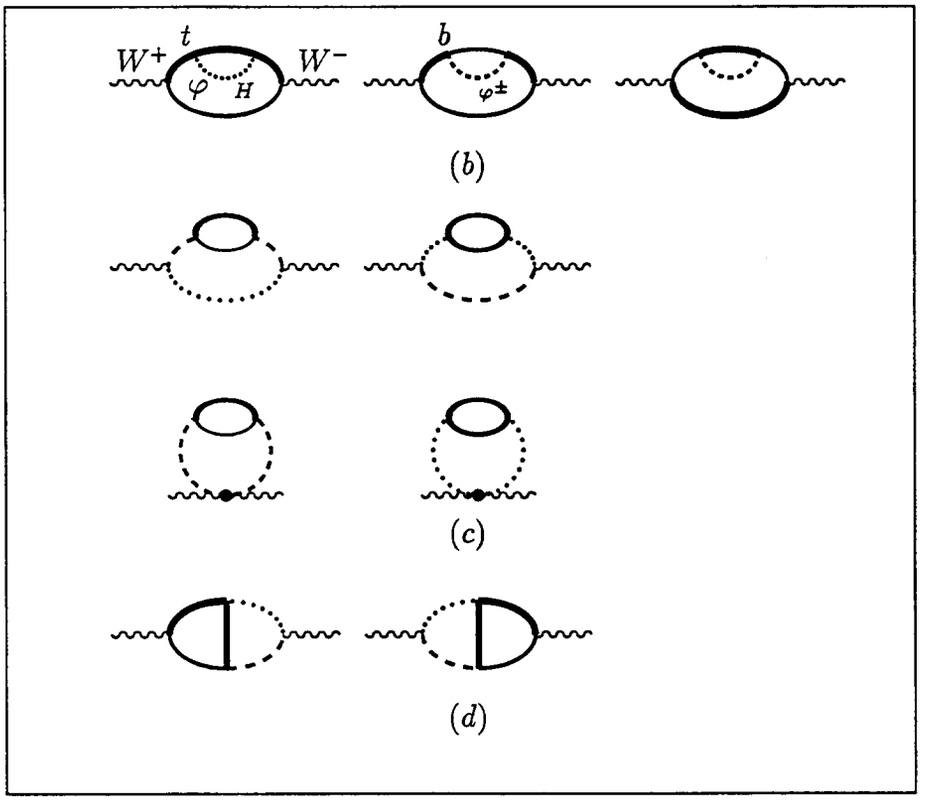

Fig. 1b: Leading 2-loop electroweak diagrams contributing to the W self-energy. Internal lines have the same meaning as in Fig. 1a.

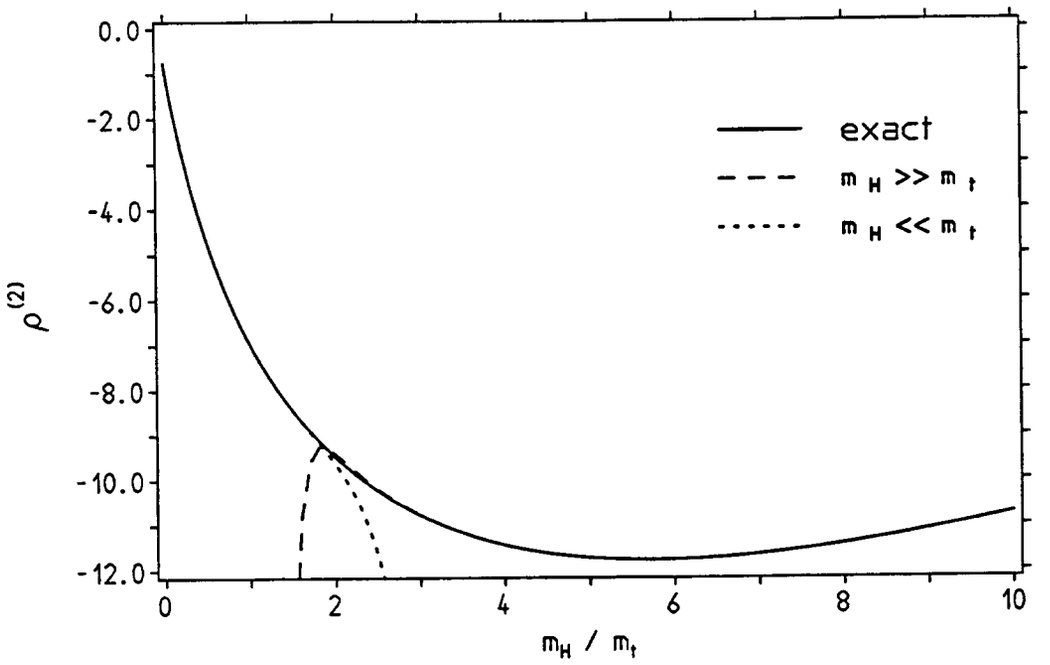

Fig. 2a: $\rho^{(2)}$ as a function of a compared with the asymptotic expansions for small and large a.

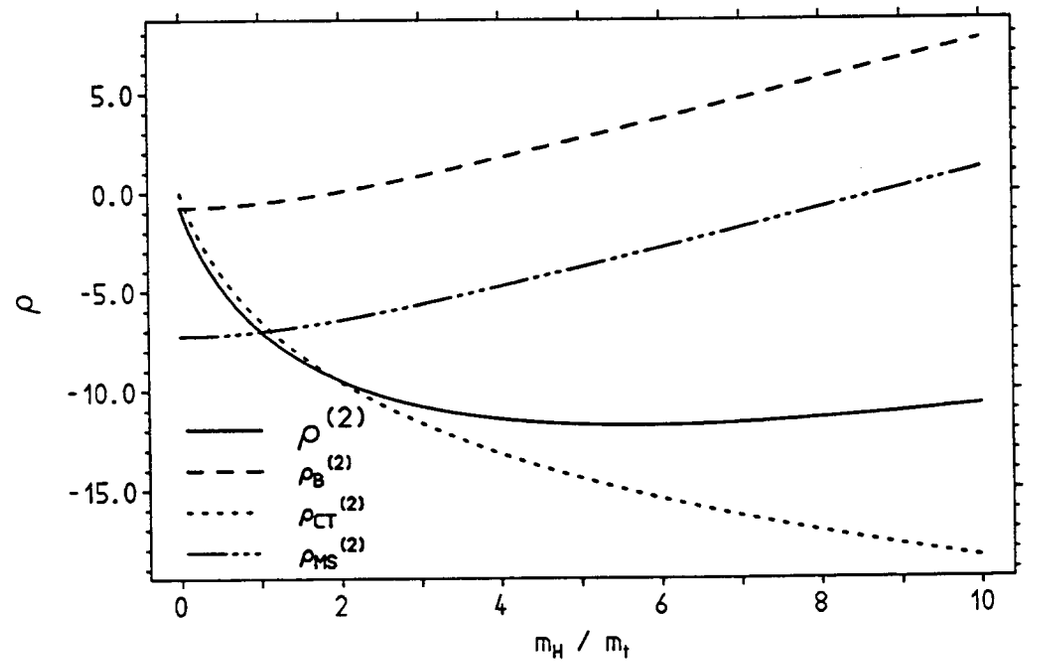

Fig. 2b: $\rho^{(2)}$ as a function of a. The bare contribution $\rho_B^{(2)}$ and the top mass counterterm $\rho_{CT}^{(2)}$, which here is subtracted at $a = 0$, are shown separately. $\rho_{MS}^{(2)}$ shows the result obtained when the $\overline{MS}$ definition is adopted for the top quark mass.

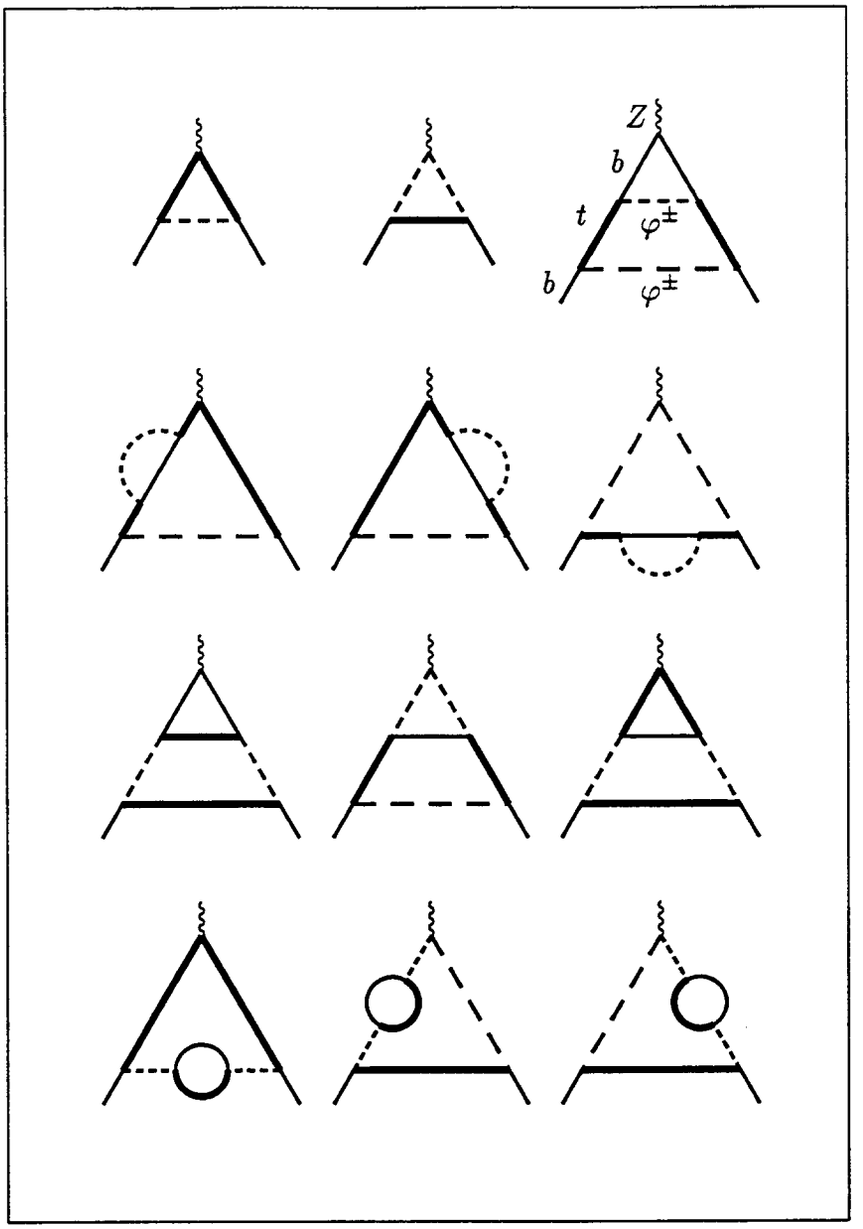

Fig. 3a: Leading electroweak loop diagrams without Higgs and neutral Higgs ghosts contributing to the $Zb\bar{b}$ vertex. Internal lines have the same meaning as in Fig. 1.

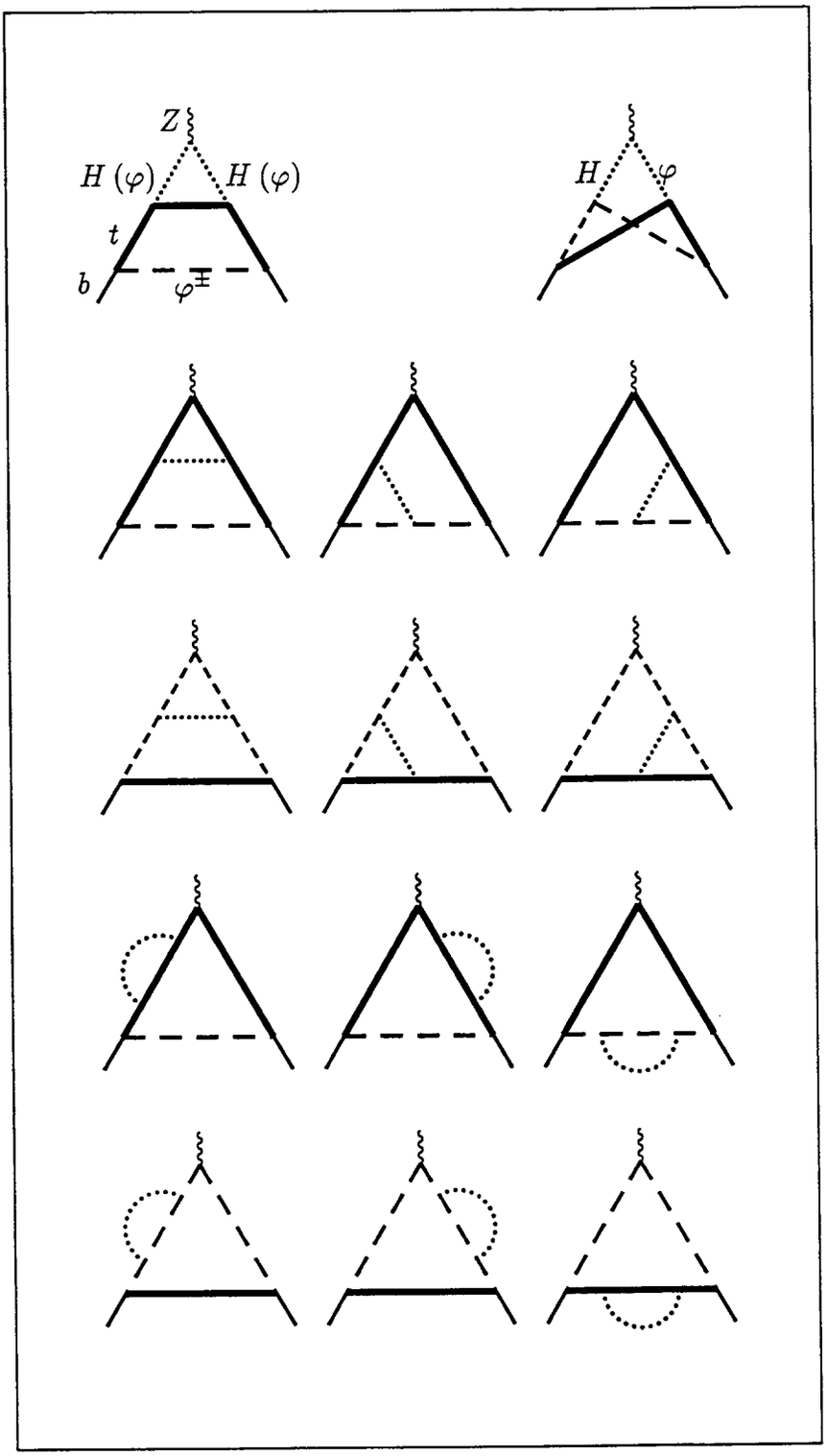

Fig. 3b: Leading 2-loop electroweak diagrams involving Higgs and neutral Higgs ghosts contributing to the $Zb\bar{b}$ vertex. Notice that φ does not couple to $\varphi^{\pm}$. Internal lines have the same meaning as in Fig. 1.

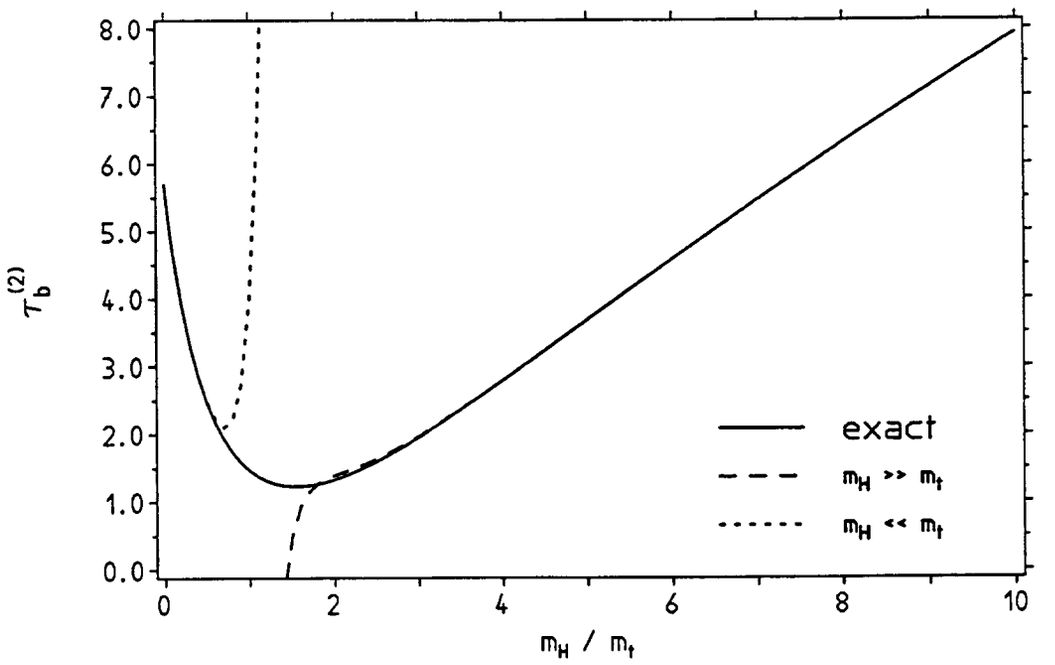

Fig. 4a: $\tau^{(2)}$ as a function of a compared with the asymptotic expansions for small and large a.

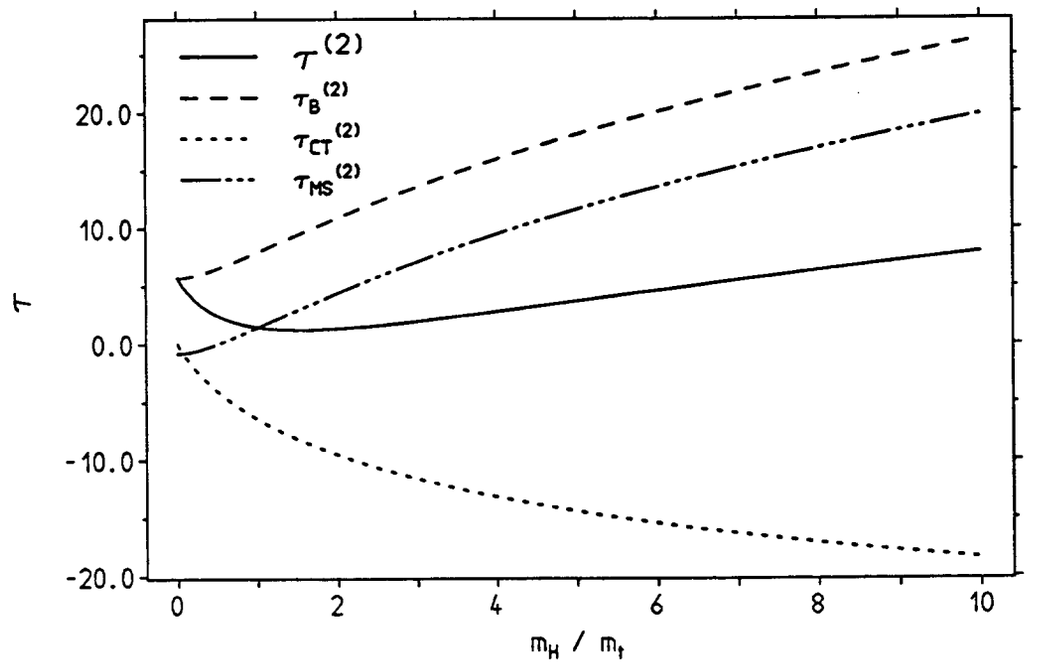

Fig. 4b: $\tau^{(2)}$ as a function of a. The bare contribution $\tau_B^{(2)}$ and the top mass counterterm $\tau_{CT}^{(2)}$, which here is subtracted at $a = 0$, are shown separately. $\tau_{MS}^{(2)}$ shows the result for the $\overline{MS}$ definition of the top quark mass.

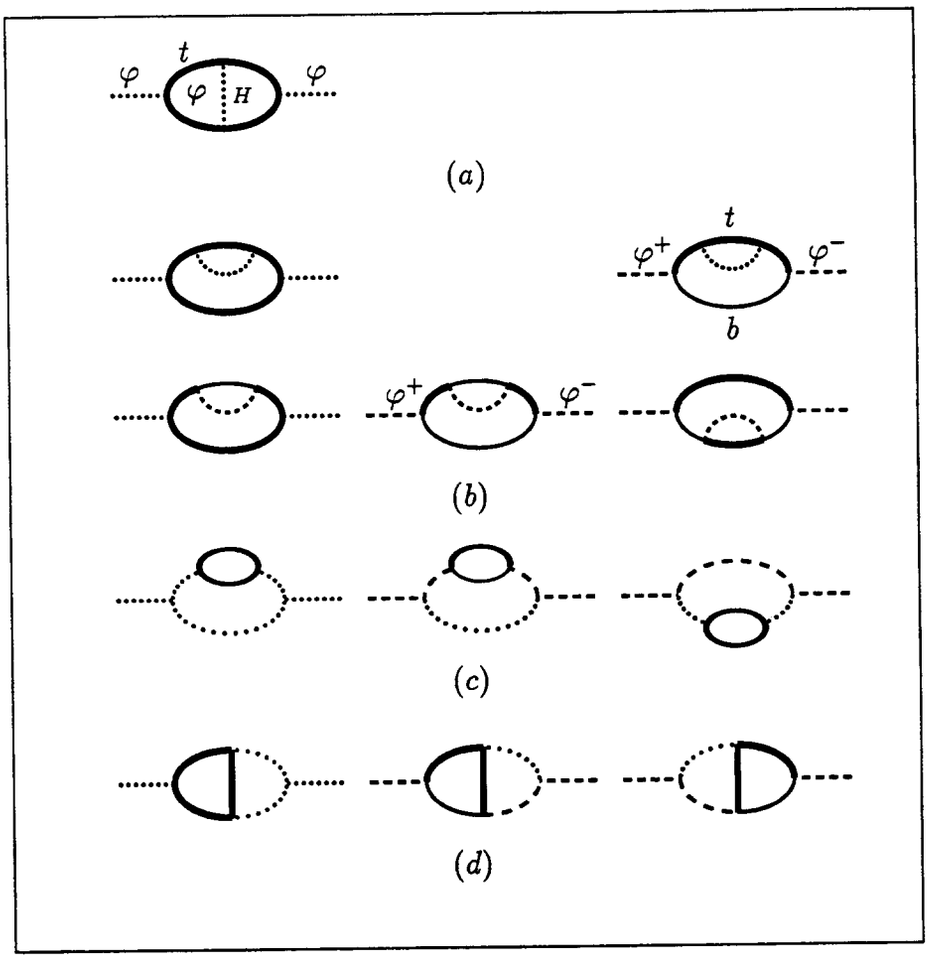

Fig. 5: Leading 2-loop electroweak diagrams contributing to the φ and $\varphi^{\pm}$ self-energy, labeled as in Ref. [8]. Internal lines have the same meaning as in Fig. 1.

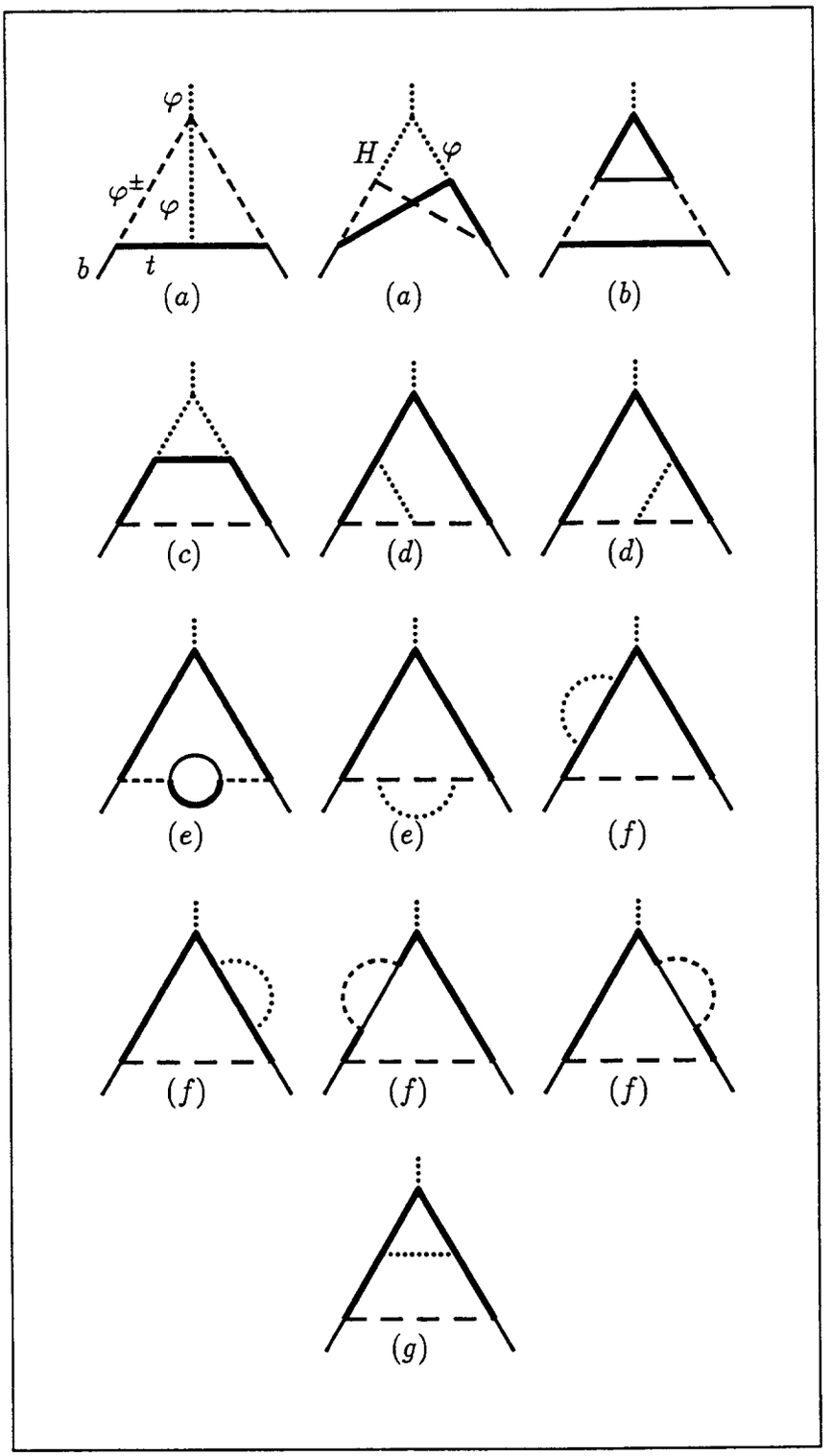

Fig. 6: Leading 2-loop electroweak diagrams contributing to the $\varphi b\bar{b}$ vertex, labeled as in Ref. [8]. Internal lines have the same meaning as in Fig. 1.

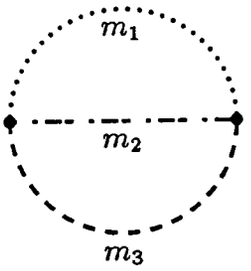

Fig. 7: General type of "bubble" diagram obtained in a heavy mass expansions at the two-loop level. In this figure each line stands for a chain of propagators of equal mass.

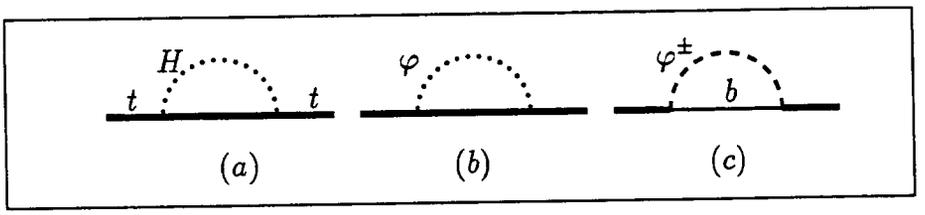

Fig. 8: Leading 1-loop corrections to the top propagator. The different lines have the same meaning as in Fig. 1.

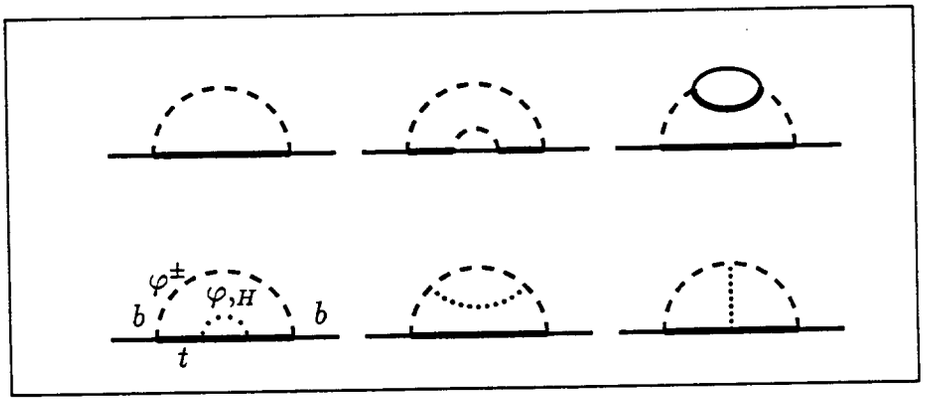

Fig. 9: Leading loop corrections to the bottom quark propagator. The different lines have the same meaning as in Fig. 1.